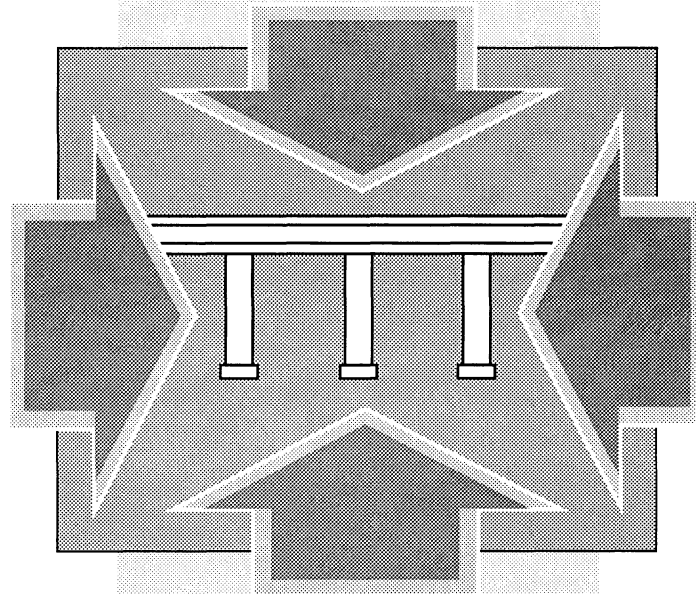


FINAL REPORT

**DYNAMIC FIELD TESTING
OF THE ROUTE 58
MEHERRIN RIVER BRIDGE**



A. L. WOLEK

Graduate Research Assistant

FURMAN W. BARTON, Ph.D.

Faculty Research Scientist

THOMAS T. BABER, Ph.D.

Faculty Research Scientist

WALLACE T. MCKEEL, JR.

Research Manager



1. Report No. FHWA/VA-97-R4	2. Government Accession No.	3. Recipient's Catalog No.	
4. Title and Subtitle Dynamic Field Testing of the Route 58 Meherrin River Bridge		5. Report Date November 1996	
		6. Performing Organization Code	
7. Author(s) A. L. Wolek, F. W. Barton, T. T. Baber, and W. T. McKeel, Jr.		8. Performing Organization Report No. VTRC 97-R4	
9. Performing Organization Name and Address Virginia Transportation Research Council 530 Edgemont Road Charlottesville, VA 22903-0817		10. Work Unit No. (TRAVIS)	
		11. Contract or Grant No. Project #3081-020	
12. Sponsoring Agency Name and Address Federal Highway Administration The Dale Building 1504 Santa Rosa Road Richmond, VA 23229		13. Type of Report and Period Covered Final Report	
		14. Sponsoring Agency Code	
15. Supplementary Notes In cooperation with the U.S. Department of Transportation, Federal Highway Administration			
16. Abstract Dynamic response has long been recognized as one of the significant factors affecting the service life and safety of bridge structures, and considerable research, both analytical and experimental, has been devoted to this area of behavior. In the design of most contemporary bridges, dynamic effects are included in the form of equivalent static loads. However, design considerations rarely include an evaluation of the structural and geometric parameters of the superstructure that influence dynamic response. Further research is needed to clarify the dynamic behavior of bridge structures and the corresponding physical characteristics that affect the response. The primary objective of this investigation was to determine and evaluate the dynamic response of a typical simple span bridge that had unexpectedly large oscillations under normal traffic loading. This was accomplished through a series of field tests in which the response was measured using accelerometers and strain gages. To supplement these data, analytical models (finite element models) representative of the bridge structure were developed to predict the dynamic response. The field data were used to validate the models. The refined models were then used for parameter studies in evaluating the effect of various factors on bridge response. The results of this investigation provided insight into the dynamic response of a typical simple span bridge constructed in accordance with AASHTO specifications.			
17. Key Words dynamic response, finite element modeling, structural dynamics, field testing, design of bridges		18. Distribution Statement No restrictions. This document is available to the public through NTIS, Springfield, VA 22161.	
19. Security Classif. (of this report) Unclassified	20. Security Classif. (of this page) Unclassified	21. No. Of Pages 37	22. Price

FINAL REPORT
DYNAMIC FIELD TESTING
OF THE ROUTE 58 MEHERRIN RIVER BRIDGE

A. L. Wolek
Graduate Research Assistant

Furman W. Barton, Ph.D.
Faculty Research Scientist

Thomas T. Baber, Ph.D.
Faculty Research Scientist

Wallace T. McKeel, Jr.
Research Manager

(The opinions, findings, and conclusions expressed in this report are those of the authors and not necessarily those of the sponsoring agencies.)

Virginia Transportation Research Council
(A Cooperative Organization Sponsored Jointly by the
Virginia Department of Transportation and
the University of Virginia)

In Cooperation with the U.S. Department of Transportation
Federal Highway Administration

Charlottesville, Virginia

November 1996
VTRC 97-R4

Copyright 1996, Virginia Department of Transportation.

ABSTRACT

Dynamic response has long been recognized as one of the significant factors affecting the service life and safety of bridge structures, and considerable research, both analytical and experimental, has been devoted to this area of behavior. In the design of most contemporary bridges, dynamic effects are included in the form of equivalent static loads. However, design considerations rarely include an evaluation of the structural and geometric parameters of the superstructure that influence dynamic response. Further research is needed to clarify the dynamic behavior of bridge structures and the corresponding physical characteristics that affect the response.

The primary objective of this investigation was to determine and evaluate the dynamic response of a typical simple span bridge that had unexpectedly large oscillations under normal traffic loading. This was accomplished through a series of field tests in which the response was measured using accelerometers and strain gages. To supplement these data, analytical models (finite element models) representative of the bridge structure were developed to predict the dynamic response. The field data were used to validate the models. The refined models were then used for parameter studies in evaluating the effect of various factors on bridge response. The results of this investigation provided insight into the dynamic response of a typical simple span bridge constructed in accordance with AASHTO specifications.

FINAL REPORT
DYNAMIC FIELD TESTING
OF THE ROUTE 58 MEHERRIN RIVER BRIDGE

A. L. Wolek
Graduate Research Assistant

Furman W. Barton, Ph.D.
Faculty Research Scientist

Thomas T. Baber, Ph.D.
Faculty Research Scientist

Wallace T. McKeel, Jr.
Research Manager

INTRODUCTION

Dynamic response has long been recognized as one of the significant factors affecting the service life and safety of bridge structures, and considerable research, both analytical and experimental, has been devoted to this area of behavior (Barton, Baber, Yen & McKeel, 1990; Fricke, 1976; Yen, 1992). Much of the attention has focused on the distribution of loads to the floor system and the determination of maximum displacements and moments, information necessary for satisfactory design (Gaunt & Sutton, 1981; Kropp, 1977). Insufficient attention, however, has been devoted to those factors that contribute to unacceptably high levels of dynamic response, thereby causing high repetitions of large displacements and stresses (Baldwin, Salane & Duffield, 1978). These conditions, in turn, may result in damage and deterioration to decks and parapets and, in some cases, to the girders themselves (Perfetti, Johnston & Bingham, 1985).

In the design of most contemporary bridges, dynamic effects are included in the form of equivalent static loads. Currently, only one formula is required for incorporating dynamic loading in the design of bridges according to AASHTO specifications (AASHTO, 1989), and the length of the bridge span is the only variable entering this calculation. This current design procedure imposes restrictions on girder depth/span ratios and static deflections (a measure of stiffness) in the hope that they will ensure satisfactory dynamic performance. These simplified design procedures can often lead to flexible structures whose response to dynamic vehicle loads may be significantly larger than that predicted by the simplified design models (Barton et al., 1990; Goble, Moses & Pavia, 1974).

Design considerations rarely include an evaluation of the structural and geometric parameters of the superstructure that influence dynamic response. Despite the extensive research

on the general dynamic response of bridge structures, the new and lighter designs, coupled with the increased use of continuous span structures and new construction procedures, have introduced several potential problems associated with dynamic response that have not been addressed. Further research is needed to clarify the dynamic behavior of bridge structures and the corresponding physical characteristics that affect the response. A well-designed and carefully planned research program, which focuses on those specific problems contributing to deck distress and/or observable motion and identifies those design and geometric parameters that are most significant in affecting dynamic response, would offer significant potential for improved dynamic behavior in new designs and enhanced behavior of rehabilitated structures.

This study was concerned with the evaluation of the dynamic behavior of a simple span bridge in Virginia that had substantial cracking in the parapets and minor cracking in the deck, indicating possible deterioration of the structure, possibly due to excessive vibration. This structure, which has a reinforced concrete deck composite with several steel plate girders, is representative of one of the major bridge types in the state, with construction completed in 1988.

PURPOSE AND SCOPE

This study had two objectives:

1. Determine and evaluate the dynamic response of a typical simple span bridge that had unexpectedly large oscillations under normal traffic loading.
2. Develop analytical models (finite element models) representative of the bridge structure that could be used to predict the dynamic response of the structure.

This study represented one phase in a continuing program of bridge testing and analysis carried out over a number of years by research engineers from the Virginia Transportation Research Council and the University of Virginia.

METHODOLOGY

The dynamic response of the bridge was determined by conducting a series of field tests in which the response was measured using accelerometers and strain gages. The loading during these field tests consisted of normal traffic loads. By appropriate analysis of these data, natural frequencies, mode shapes, and damping characteristics were determined.

Analytical models (finite element models) representative of the bridge structure were developed that could be used to predict its dynamic response. The field data were employed to

validate the computer models, and these refined models were then used for parameter studies in evaluating the effect of various factors on bridge response.

Test Structure

The bridge used as the test structure is located in Brunswick County, Virginia, approximately 0.8 km (0.5 mi) west of State Route 644, and carries the eastbound lanes of Route 58 over the Meherrin River. The traffic volume is moderate, but heavy vehicles, such as logging trucks, frequently use the bridge. The structure was replaced in 1988, and the replacement structure was designed in accordance with AASHTO specifications and modifications by the Virginia Department of Transportation. The design load used was HS20-44 and alternate military.

The bridge superstructure consists of three spans, each simply supported and consisting of a reinforced concrete slab on four steel girders. The center span is 32.5 m (106 ft, 6 in) in length, and the side spans are each 14.7 m (48 ft, 3 in) in length. Figure 1 shows an elevation view of the bridge, and Figure 2 shows a transverse section. The concrete deck is 21.6 cm (8.5 in) thick, and approximately 5 cm (2 in) of concrete elevates the deck above the girders. Since only the center span had an excessive dynamic response, the side spans were not included in this study. Although not apparent in the figure, eastbound traffic on Route 58 has a steep down grade just before the bridge. This geometric feature causes an increase in the horizontal and vertical velocities of the vehicles approaching the bridge.

NOTE: All of the figures cited in this report may be found in the Appendix.

Test Equipment

Primary test equipment included two types of transducers, a data acquisition system, and analysis equipment. The transducers employed were accelerometers and strain gages used to measure actual accelerations and strains during the tests. The data acquisition system provided power to and gathered signals from the transducers. It also reduced, converted, and recorded signals for future processing. The system used was the Megadac 2210C Data Acquisition System from Optim Corporation. The system included a tape drive for data storage and various ports for communication with other digital devices.

The data obtained from the field tests were available in both digital and analog form. In analog form, the data were analyzed using FFT signal analyzers. In digital form, the data were analyzed using digital computers and software packages designed for such use. Two FFT signal analyzers were used in this study: an Ono Sokki CF-200 portable field FFT analyzer and an Ono Sokki CF-350 portable dual channel FFT analyzer. Digital signal processing software, using fast

Fourier transform analysis, was used for computational analysis of the data on an IBM-compatible DOS PC.

Instrumentation Plan

Ten accelerometers and six strain gages were positioned on the deck at the locations indicated in Figures 3 and 4. The accelerometers were placed at the 1/4, 3/8, 1/2, 5/8, and 3/4 lengths of the span, and the strain gages were installed at the quarterspan and midspan and at the location where the bottom flange changed thickness. The accelerometers and strain gages were placed directly over the exterior girder within the shoulder area of the span. The longitudinal location (x coordinate) of each transducer as measured from the west pier is given in Table 1. The accelerometer locations were based on an estimate of the vibration modes of the girders as predicted by a preliminary finite element model analysis of the bridge.

Table 1. Longitudinal Location of Transducers Measured from West Pier

Channel	Transducer Type	X Location (m)
0	Accelerometer	8.11
1	Accelerometer	12.17
2	Accelerometer	16.23
3	Accelerometer	24.34
4	Accelerometer	8.11
5	Accelerometer	12.17
6	Accelerometer	16.23
7	Accelerometer	24.34
8	Accelerometer	20.29
9	Accelerometer	20.29
10	Strain gage	6.10
11	Strain gage	8.11
12	Strain gage	16.23
13	Strain gage	8.11
14	Strain gage	16.23
15	Strain gage	6.10

The largest strains were expected at the midspan. Data from gages at the quarter span would indicate any effects of the nonuniform bottom flanges and serve to confirm mode shapes extracted from the accelerometer data. The strain data also provided a basis for comparison with strains predicted by the finite element models. The analytical predictions of strain were obtained by extracting displacements from the acceleration data and then loading the finite element models with these derived displacements.

Data Recording and Reduction

Data recording was essentially the same for all field tests. Sixteen channels of data were recorded simultaneously on the Megadac system. The first 10 channels were used for accelerometer signals, and the last 6 for the strain gage signals. A sampling rate of 100 Hz was used, which allowed the extraction of frequencies up to almost 50 Hz. Nineteen runs were made, with each starting just before a large truck entered the bridge and lasting several minutes.

Data were stored on magnetic tape and later transferred to floppy disks. Preliminary analysis of the data indicated that the dominant frequencies were all less than 25 Hz, and, thus, only the first run was stored at the full 100 Hz sampling rate. The data for the remaining runs were transferred and stored at a sampling rate of 50 Hz. This reduced the amount of storage space required and allowed longer records to be analyzed on the computer.

RESULTS AND DISCUSSION

Experimental Results

Accelerations and strains recorded during the various field tests were evaluated and analyzed to determine the natural frequencies, mode shapes, and other dynamic response characteristics of the test structure. Data were reduced and processed using an FFT analyzer and a software package, DADiSP, specifically developed for data analysis on a PC. Only 9 of the 10 accelerometer channels were used since accelerometer 7 malfunctioned during the initial field test.

A relatively simple computer model of the bridge was used to identify the approximate mode shapes corresponding to the bridge's natural frequencies. The first 12 mode shapes and frequencies developed from this model are shown in Figure 5. The first mode is the first bending mode of the bridge, the second is the first torsional mode, the third is the second bending mode, and the fourth is the second torsional mode. Experimental data indicated that higher modes corresponding to frequencies above 15 Hz produced very low acceleration and strain values and, therefore, would be expected to produce almost negligible stresses.

A typical accelerometer time record, measured from accelerometer 1, for a part of one run is shown in Figure 6. A frequency response plot corresponding to this accelerometer record is given in Figure 7. All frequencies determined from this frequency response plot are listed in Table 2. The dominant response frequency was 2.7 Hz, which appeared to be the first bending mode. Other modes appeared to contribute little to the bridge response for this run.

Table 2. Relative Frequency Amplitudes from Acceleration Spectrum

Channel	F1 = 2.73 Hz	F2 = 3.22 Hz	F3 = 9.62 Hz	F4 = 10.16 Hz	F5 = 12.5 Hz
0	.005 G	.0012 G	.0011 G	.0007 G	.0003 G
1	.0062 G	.0014 G	.0007 G	.0005 G	.0003 G
2	.0063 G	.0015 G			.0004 G
3	.0044 G	.001 G	.001 F	.0006 G	.0003 G
4	.0044 G	.0011 G		.0004 G	.0003 G
5	.0058 G	.0014 G			.0004 G
6	.0066 G	.0018 G			.0004 G
8	.0061 G	.0014 G	.0006 G	.0005 G	.0004 G
9	.0062 G	.0015 G		.0003 G	.0004 G

It was felt that certain of the frequencies might have been the result of vehicle-structure interaction and represented natural frequencies of the truck. In an attempt to minimize or eliminate this effect, the total acceleration record was separated into two parts, a so-called transient phase while the vehicle was traversing the span, and a free vibration phase immediately following the passage of the truck. The acceleration records corresponding to the transient phase and the associated frequency response are shown in Figures 8 and 9, respectively, and the same plots for the free vibration phase are shown in Figures 10 and 11. The frequency response spectrum in Figure 9 shows a strong frequency component at 4.6 Hz, which does not appear in the spectrum for the free vibration portion of the record. This is apparently one of the vehicle frequencies, or at least a result of vehicle-bridge interaction. It is important to separate out the load-structure interaction frequencies from the natural frequencies of the bridge before attempting to identify the mode shapes corresponding to the bridge frequencies.

A number of methods are available for identifying the various vibration modes from acceleration data. The symmetry of this structure made it possible to employ basic methods. For example, because of symmetry, the two accelerometers at either the midspan or quarterspan should indicate essentially identical responses in the first bending mode. For the same reason, the two midspan accelerometers should be 180 degrees out of phase in the first torsional mode. Therefore, if the acceleration record formed by the difference between the response of

accelerometers 2 and 6 is transformed to the frequency domain, the corresponding spectrum should represent a response in which the first bending mode is eliminated and the first torsional mode is magnified. This response spectrum is shown in Figure 12. The first torsional mode is at 3.2 Hz, and the first bending mode at a frequency of 2.7 Hz was essentially eliminated.

Similarly, the second torsional mode can be more easily identified by subtracting the signals from the two quarterspan accelerometers and examining the resulting frequency spectrum. The response spectrum formed in this way is shown in Figure 13, which indicates that the second torsional mode corresponded to a frequency of approximately 10.2 Hz. This figure also confirms the previously determined frequencies for the first torsional and bending modes. Also, as may be observed, the amplitudes of both longitudinal bending modes were significantly reduced. The second bending mode is clearly indicated at 9.6 Hz, which is about 0.5 Hz lower than the second torsional mode. The simple computer model also predicted the second bending mode at about 0.5 Hz lower than the second torsional mode, and the prediction of the first torsional and first bending frequencies from this simple model also compared favorably.

An FFT analyzer was also used to determine the natural frequencies of the structure from the accelerometer data and provide a check on the response quantities determined from the data analysis software package. Output from the Ono Sokki dual channel FFT analyzer showing the response spectrum corresponding to the acceleration record from accelerometer 0 is shown in Figure 14. The significant frequencies compare well with those determined from the digital computer software. Figure 15 is a cross-spectrum phase plot between channel 0 and channel 4. As expected, the two frequencies generated are the same first and second torsional modes derived by the subtraction method.

The contribution of the first bending mode to the total response was about 5 times greater than that of the next largest mode (for most signal samples), and this mode shape produced the largest longitudinal midspan stresses. This was based on acceleration data. Strain data indicated the first bending mode to be even more significant. The measured strains from a gage located at the midspan during a typical test run is shown in Figure 16. The large initial strain possibly signifies a large impact and/or a very large load. This was also observed in the accelerometer data for an accelerometer located at close proximity to the gage for that particular run. Figure 17 shows the response spectrum for this strain gage record. The initial peak at less than 1 Hz is likely a result of the speed effect of the truck. This frequency plot also shows clearly the fundamental frequency of 2.7 Hz corresponding to the first bending mode.

Although it was not possible to measure displacement directly, it was hoped that successive integration of the accelerometer signal would provide a reasonable measure of displacements. It might then be possible to relate these displacements to the stresses. Figure 18 indicates the displacement response obtained from a double integration of the acceleration record for a short time interval. For comparison, the measured strain response from a strain gage at the same location as the accelerometer is shown in Figure 19, and, as may be observed, the comparison was quite good. However, determining displacements by double integration of an

acceleration signal appears to work consistently only for very short time samples. As sample length increases, the integrated signal develops skews and other random effects because of the accumulation of errors. These errors originate from the transducers and the data acquisition system as well as unknown initial conditions and possibly the sample rate. For very short samples, simple regression techniques seem to limit these errors to an acceptable level.

The displacement data generated through integration of accelerations were subsequently applied as the loading to the finite element computer models to provide stress data. These data were then compared with stress data derived from the strain transducers. This allowed not only a rough check to be made on the accuracy of the equipment and method, but also an estimate of stresses in the least accessible parts of the bridge, such as the bottom flanges.

Response data also permitted consideration of whether any conclusions could be made regarding impact. In bridge design, the effect of vehicle impact on bridge structures is accounted for by using the AASHTO impact formula, which is a function of only the span length. Although this approach has been shown to be adequate for most bridges, there are certain situations in the case of long span structures and/or heavy vehicle loads where impact may be underestimated. In this investigation, an attempt was made to estimate impact by comparing the dynamic strain response to the static strain response. However, the recorded strains obtained from gages on the deck were so small that no meaningful conclusions on impact could be made.

Damping was also of interest, and damping was estimated by the logarithmic decrement method. The resulting linear viscous damping ratio was calculated for the first bending mode amplitudes of accelerations and strains. The first mode had the most significant amplitudes of vibration and was thus expected to dissipate much more energy through damping than other modes. The linear viscous damping ratios are provided in Table 3 for five selected test runs. Midspan accelerometer and strain gage data were used for the calculations. The average damping value based on the data in Table 3 was approximately 0.6 percent, indicating relatively low damping for this bridge. It was noted from field observations that the bearings supporting the superstructure seemed to be frozen during dynamic response. Since damping is at least partially obtained through the mobilization or the elastic action of bearings, the lack of action of the bearings on this bridge may have contributed to the low damping values obtained.

Analytical Investigation

This analytical phase of the study was concerned with the development of finite element models of the bridge and an evaluation of the dynamic response of these models. A comparison of predicted and measured responses was used to refine the models and develop final models of the bridge that could provide reliable dynamic response information. Relatively simple models

Table 3. Typical First Mode Damping Data Based on Strain and Acceleration Signals

Signal File No./Channel	Value	Time 1 (sec)	Value 2	Time 2 (sec)	No. of Cycles	Damping (%)
19/2	.0997 G	7.22	.0597 G	11.64	12	0.7
20/2	.1103	61.6	.0795	66.02	12	0.4
23/2	.148 G	9.3	.112 G	11.52	6	0.7
24/2	.0988 G	8.12	.0829 G	9.6	4	0.7
26/2	.135 G	9.8	.1025 G	12.02	6	0.7
19/12	49 UE	7.4	47.7 UE	9.62	6	0.7
20/12	52.5 UE	67.12	51.4 UE	70.8	10	0.3
24/12	20.9 ue	8.3	20 UE	9.78	4	0.5
26/12	48.4 UE	9.98	45.3 UE	12.2	6	0.8

were studied initially to develop insight into the complexity and degree of sophistication of the model necessary to provide reliable and accurate predicted responses. Additional modeling details were added as necessary with the idea that the best model to be used for predicting response would be the simplest model that could provide accurate results. The finite element code ANSYS was used in all of the analyses.

After a number of preliminary studies in which beam models and very simplified finite element models were evaluated, a finite element model of the complete centerspan structure was developed and is shown in Figure 20. The primary purpose of developing this model was to provide reliable estimates of mode shapes and frequencies for the entire bridge. Parameter studies were also performed on this model, which is subsequently referred to as the MES model.

For this model, pinned or simply supported boundary conditions were used on one end and roller boundary conditions were used on the other. Master degrees of freedom (MDOF) for the frequency extraction were selected to be along the outside girders since the accelerometers were also located along those girders.

The slab, girder, and diaphragm components were represented by three-dimensional shell elements. The concrete deck was represented by an interior and exterior region in which the exterior region was assigned increased density to account for the dead load of the barrier. The girder webs were connected directly to the slab, and no representations of the upper flanges were used to reduce the size of the model. A slightly larger modulus of elasticity was used for the concrete in the deck to account for the presence of the upper flange. The modulus of elasticity also reflected the steel reinforcement in the deck. Intermediate and end diaphragms were modeled using plate elements of the same thickness as the web stiffener plates and were

connected to the web elements. Two geometries were used for the bottom flanges to represent the nonuniform bottom flange in the actual structure. This particular model had 441 nodes and 418 elements. Variations of this model, using different representations of the diaphragms and different MDOFs, were also evaluated. The mode shapes and frequencies based on this model representation, including the diaphragms, are presented in Figure 5.

Deleting the diaphragms from the model had a significant effect on the torsional frequencies. The first 10 frequencies and mode shapes for a model without diaphragms are shown in Figure 21. By comparing these results with those in Figure 5, it is observed that the torsional mode frequencies preceded the bending mode frequencies for both the first and second modes in this model. As a result, since intermediate diaphragms contribute substantially to the torsional stiffness of the structure, they were included in subsequent models.

Because of the sensitivity of the torsional and transverse bending frequencies to the presence of the diaphragms, a proper representation of the diaphragms in the computer model was essential. This was accomplished by adjusting the model until those predicted frequencies most sensitive to the diaphragms compared closely with the measured values. The first transverse bending mode was particularly sensitive to the diaphragms, and this mode was selected as a basis for comparison. The experimentally measured frequency for this mode was 12.5 Hz, as indicated in Table 2. This frequency was originally overestimated by the computer model. The representation of the diaphragms was modified until the predicted analytical frequency matched the experimental value of 12.5 Hz. The first six frequencies of this model, with proper representation of the diaphragms, are given in Figure 22. These predicted frequencies compared very closely to the frequencies measured experimentally, especially for the first five modes. Predicted frequencies were obtained using 30 MDOF, 10 along each of the exterior girders, and 10 along the longitudinal centerline.

The results from the analytical model indicated that it is possible to develop finite element models that can accurately predict natural frequencies of actual structures. If sufficient dynamic data are available from field tests of the actual structure, different components of the computer model may be refined and modified to represent better the corresponding structural members in the real structure.

A more detailed model of a portion of the bridge superstructure was developed by considering only one girder line of the structure. An interior girder line was selected since a larger contribution of live load would be expected along the interior girders. Such a detailed modeling permitted the effects of dead and live loads to be analyzed in specific locations of the cross section, such as the top flanges, which is not possible in the model of the entire structure. Displacements attributable to dynamic loading, obtained through a double integration of the acceleration data, may be easily applied to this model.

Two representations of the slab and girder interface were used to evaluate the force transfer between the concrete deck and steel girder. The first employed a layered element to

represent the deck-flange connection. In this model, the girder web was connected to two concrete layered elements, as shown in Figure 23. These are the only layered elements in the element connectivity pattern shown in Figure 24. All other elements are plate elements. The pattern is repeated to produce the girder line model shown in Figure 25 in which there are 250 eight-node elements.

There are five layers in the two special elements. The top two are nonstructural (small Young's modulus) and exist to allow the middle concrete deck layer to be in the same geometric plane as the other concrete deck elements. The fourth layer is equivalent to the 5 cm (2 in) of concrete that elevate the slab above the top flange. The flange is the fifth layer. As a result, the girder web first transfers the force to the middle layer, which is the deck. A part of the load is then transferred to the 5-cm (2-in) concrete interface, and eventually to the steel flange. The second representation assumed the load was first taken by the top flange and the concrete interface and then transferred to the deck elements. The element connectivity pattern for this model is shown in Figure 26, and all the elements are of the same type. The stiffness of the interface between the deck and flange was controlled by changing the width of the interface element. There were 325 four-node elements in this model. These two models are referred to as SG1 and SG2, respectively, in the following discussion.

Finally, a detailed model of one-quarter of the bridge, designated the QBM model and shown in Figure 27, was developed, which allowed both dynamic and static analysis to be performed. The model was made symmetric about the two edges by using proper boundary conditions, making it possible to represent the behavior of the full bridge structure yet use only one-quarter of it for analysis. This approach, however, obviously restricted the predicted response to symmetric behavior. A total of 406 four-node elements were used in this model.

The representations of the girders and slab are shown in Figure 27. There are three diaphragms between the two girder lines. These cannot be seen in their entirety since the element plot uses a hidden line removal algorithm. There are three half-diaphragms that can be seen that terminate at the symmetry plane. The slab/girder interface is produced by using two diagonal plate elements for each girder line.

Using symmetric boundary conditions, the mode shapes symmetric about the two symmetry planes were extracted from the QBM model. The first two of these modes, which correspond to the first longitudinal bending mode (2.7 Hz) and the first transverse bending mode (12.5 Hz) for this symmetric model, are shown in Figures 28 and 29. The first transverse mode was very sensitive to the diaphragm stiffness. The diaphragms act as beams in the transverse direction, although they are not connected rigidly to the slab. The elastic modulus of the diaphragms was modified until the 12.5 Hz frequency was obtained, which matched the 12.5 Hz frequency of the actual bridge. This required a reduction in the diaphragm modulus from an initial value of 206.7 GPa to 63.4 GPa (30E6 to 9.2E6 psi), which produced insignificant changes in the other frequencies.

Using this QBM model, other modes and frequencies could be identified through the proper use of boundary conditions. For example, by specifying asymmetric boundary conditions at the end of the model (half-span of full bridge) and symmetric boundary conditions at the side (half-width of full bridge), a frequency that corresponded to the second bending mode was determined to be 9.7 Hz. This is essentially the same as the experimentally measured frequency of 9.6 Hz for the same mode, which is shown in Figure 30. Using a different set of boundary conditions, another mode was extracted at 16.3 Hz and is shown in Figure 31. This was close to the measured frequency of 16.5 Hz, which corresponded to the sixth mode shape in Figure 5.

Evaluation of Analytical and Experimental Results

Static Loads

Before a dynamic analysis, the finite element models were used to determine dead and live load static stress levels within the structure. The two detailed single-girder line models were used first. By applying the same live load to the SG1 and SG2 models, which differed only in the interface modeling, the different interface representations could be evaluated. The live load used was the AASHTO maximum and was equivalent to 80.1 kN (18,000 lb) concentrated at the midspan and 9.34 kN/m (640 lb/ft) distributed along the span. Since these loads are for one lane, the actual applied live loads were one-half of these values.

These static loads were applied to the two girder models, and the analytical results showed that the stiffnesses of the two models compared closely. The maximum deflection for the SG1 model was 16.8 mm (0.66 in), and that for the SG2 model was 15.7 mm (0.62 in). The maximum stresses in the bottom flange were also in close agreement, 2.58 MPa (3,750 psi) for the SG1 model and 2.54 MPa (3,680 psi) for the SG2 model. A stress profile for the bottom flange of the SG1 model is shown in Figure 32, and a similar plot for the deck stresses is shown in Figure 33. In Figure 32, the discontinuity indicated in the bottom flange stresses was a result of the change in flange thickness. The displacement plot along the span is given in Figure 34 for the SG1 model. Changing the dimensions of the interface element in the SG2 model had a negligible effect on stress and displacement results.

To estimate dead load stresses, it was assumed that only the girder resisted the dead load. This was accomplished in the model by reducing the stiffness of the concrete. Since the SG1 model used the concrete for load transfer to the top flange, the SG2 model was used for this calculation.

For the dead load acting on the steel girder, the model predicted an average maximum compressive stress of 124.7 MPa (18,100 psi) in the top flange at the midspan and an average maximum tensile stress of 79.9 MPa (11,600 psi) in the bottom flange. The dead load stresses calculated using the AASHTO procedures (referred to as theoretical) were 125.4 MPa (18,200 psi) compression for the top flange and 80.6 MPa (11,700 psi) tension for the bottom flange. The

calculated stresses compared very favorably with those predicted by the finite element model. Both the theoretical and computer solutions indicated a maximum dead load deflection of approximately 10.2 cm (4 in). The results described were for a typical interior girder.

The maximum allowable stress in the steel is 189.5 MPa (27,500 psi). This assumes that lateral support is present during the pour. The steel reinforcement, which is usually tied to the shear studs, and the intermediate diaphragms are assumed to provide adequate lateral support at this stage of construction. The maximum allowable compressive concrete stress is 11 MPa (1,600 psi). Based on these results, it may be concluded that the total dead and live load steel girder stresses and the concrete stresses attributable to live loads were well within the AASHTO allowable stress bounds.

Dynamic Stresses

To provide an estimate of the stresses produced in the bridge as a result of dynamic response, approximate displacements calculated from measured accelerations were applied as loads to the corresponding nodes of the finite element models. Stresses produced by these applied displacements were then assumed to be the actual dynamic stresses resulting from traffic loading. These stresses were then compared with the stresses obtained from actual strain data for verification. Three computer models, the QBM, SG1, and SG2 models, were used for this analysis. The displacements determined from integration of the experimental accelerations served as the input displacements to the models. The stresses from the computer models and those calculated from measured strain data were compared at the midspan since the largest longitudinal stresses were expected at that location.

Since the QBM model simulates one quarter of the bridge, the displacements along the outside girder were as given by channels 0, 1, and 2. The displacements along the interior girder lines were interpolated values between channels 4 and 0, channels 5 and 1, and channels 6 and 2. Symmetry boundary conditions were used along the appropriate edges. The midspan stresses produced by this model were 9.3 MPa (1,354 psi) tensile in the bottom flange and 1.6 MPa (238 psi) compressive in the concrete deck.

The SG2 model used channels 0, 1, 2, 8, and 3 for displacements along the corresponding position on the span. For the bottom flange, the model gave a tensile stress of 10.5 MPa (1,517 psi). The concrete stress was 1.1 MPa (164 psi) compressive.

A modified approach was used for the SG1 model. Deck and bottom flange stresses and displacements for this model are shown in Figures 32, 33, and 34 for the case of applied live loads. A factor of 2.46 was used to scale down the midspan live load deflection to correspond to the dynamic deflection. The same factor was then used to scale down the stresses. This assumed that the stress-displacement relationship is linear. The resulting midspan bottom flange stress

was 10.5 MPa (1,524 psi) tensile, and the concrete deck stress was 2.4 MPa (354 psi) compressive.

The experimental concrete deck stress was approximately 1.4 MPa (200 psi), based on an average of maximum recorded strains and using an elastic modulus of approximately 24.8 GPa (3.6 E6 psi). The average value of the stress from the three computer models was approximately 1.7 MPa (250 psi). These were judged to be good comparisons. Further, it is anticipated that averaging the bottom flange stresses for the three models will give a good estimate of the actual bottom flange stress. The average was 10.1 MPa (1,465 psi).

CONCLUSIONS

- The results from this investigation provided insight into the dynamic response of a typical simple span bridge constructed in accordance with recent AASHTO specifications. The information provided herein would be of use to bridge engineers concerned with new construction as well as those engineers concerned with possible retrofits to reduce dynamic response.
- A systematic and accurate experimental procedure was established that provided information on the dynamic response of the instrumented bridge superstructures subject to random types of loads. This procedure used acceleration and strain transducers. The qualitative response output from the strain transducers was compared with displacements obtained directly through integration of acceleration data. The strain gage data were also compared with accelerometer data by using finite element computer models. Spectrum analyzers were used to check results obtained by using FFT software on a digital computer. These comparisons proved all of the components of the experimental procedure to be functioning correctly.
- Computer models using shell elements worked very well for simulation of the slab on girder composite bridge structures. Moreover, different parts of the models were isolated and modified to represent the actual structure better. These detailed models provided information on the parts of the structure that were not instrumented because of lack of access and/or lack of extra transducers.
- Static design methods neglect the rebound from dynamic loading, which places the concrete deck in a state of tension after the initial compressive response. This reversal of stresses continues during the free vibration of the damped structure. However, during the transient response, that first tensile stress may reach levels close to the initial compressive stress. This may lead to deterioration and cracking of the deck and parapet.

- Experimental and analytical results suggest that exterior girders may experience much larger strains than interior girder lines. This was true for the test bridge where torsional modes of vibration were significant.
- All of the dominant natural frequencies for this structure were within the frequency range of 2 to 5 Hz.
- Structural damping for this bridge was very low, approximately 0.5 percent. Bearings on the bridge, which appeared to be frozen during the dynamic response, may account for the low damping of this structure.

REFERENCES

- AASHTO. (1989). *Standard Specifications for Highway Bridges*. Washington, DC.
- Baldwin J.W., Jr., Salane H.J. & Duffield R.C. (1978). *Fatigue Test of a Three-Span Composite Highway Bridge*. Missouri State Highway Department Study 73-1.
- Barton F.W., Baber T.T., Yen W.-H. & McKeel W.T. Jr. (1990). *Dynamic Field Test of a Flexible Simple Span Bridge*. Proceedings of the Third International Conference on Bridges. Toronto.
- Fricke H.F. (1978). *Traffic-Induced Dynamics of Highway Bridges*. Master's Thesis, University of Nevada at Reno.
- Gaunt J.T. & Sutton C.D. (1981). *Highway Bridge Vibration Studies*. Joint Highway Research Project by Purdue University and Indiana State Highway Commission. FHWA/IN/JHRP-81/11.
- Goble G.G., Moses F. & Pavia A. (1974). *Field Measurements and Laboratory Testing of Bridge Components*. OHIO-DOT-08-74. Ohio Department of Transportation.
- Kropp P.K. (1977). *Experimental Study of the Dynamic Response of Highway Bridges*. Doctoral Dissertation, Purdue University.
- Perfetti G.R., Johnston D.W. & Bingham W.L. (1978). *Incidence Assessment of Transverse Cracking in Concrete Bridge Decks: Structural Considerations*. FHWA-RD-87/059. North Carolina Department of Transportation.
- Yen W-H. (1992). *Modal Identification of Bridge Structures*. Doctoral Dissertation, University of Virginia.

Appendix

FIGURES

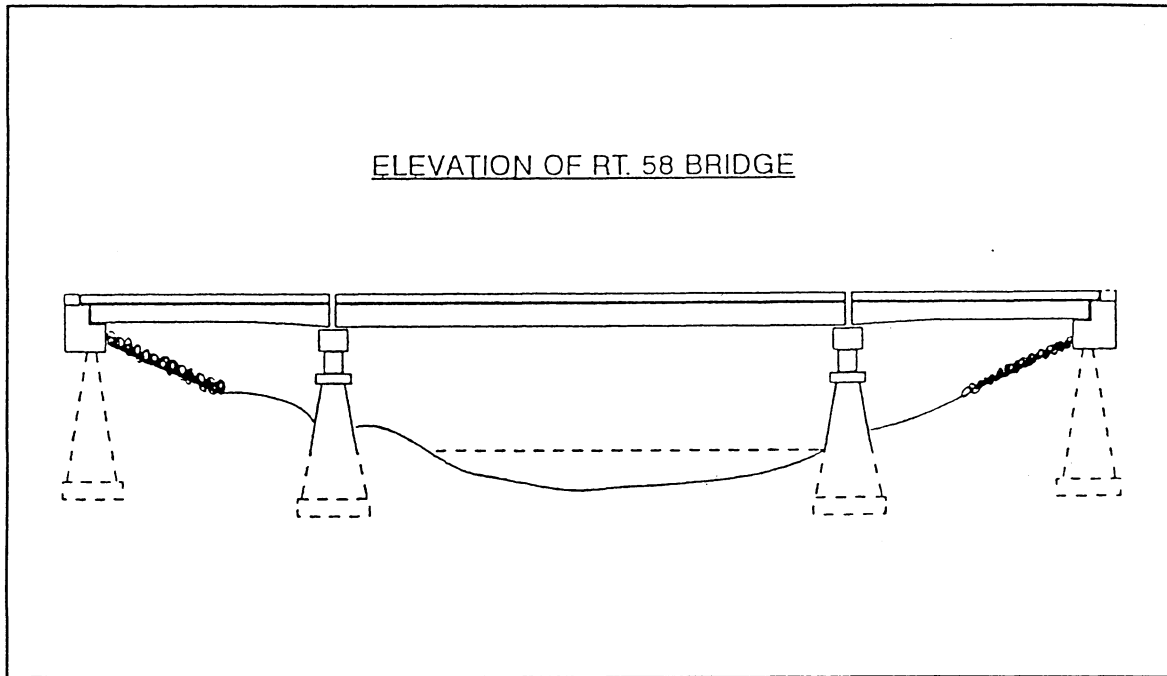


Fig. 1 Elevation View of Route 58 Bridge

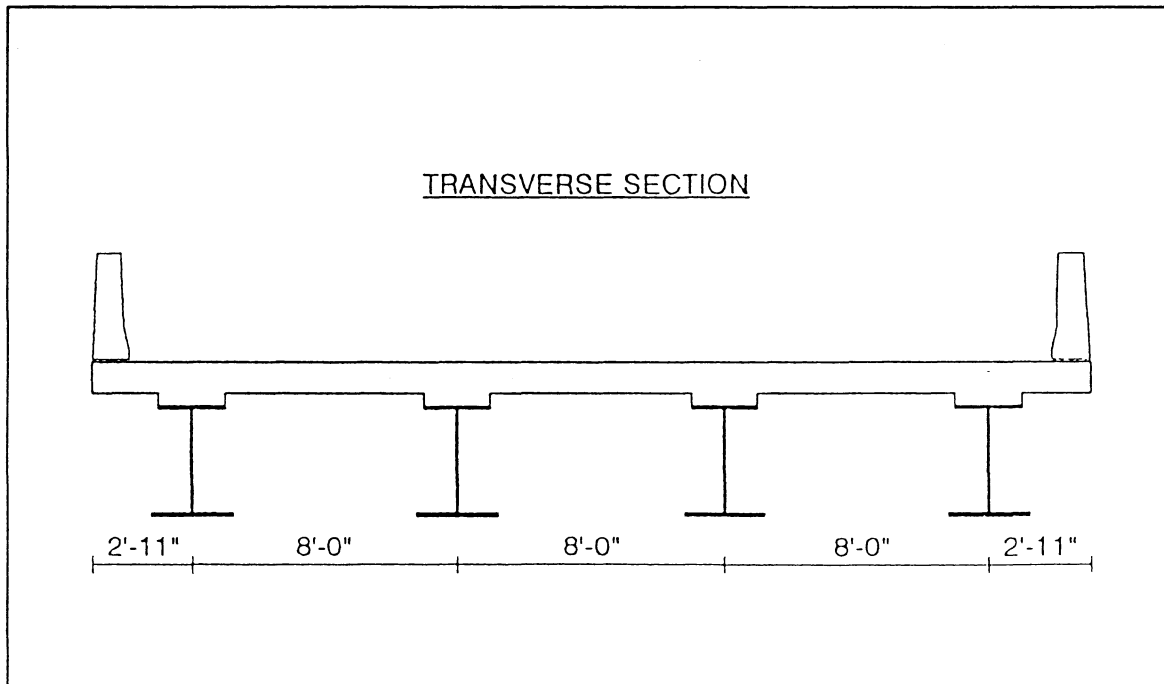


Fig. 2 Cross-Section of Superstructure

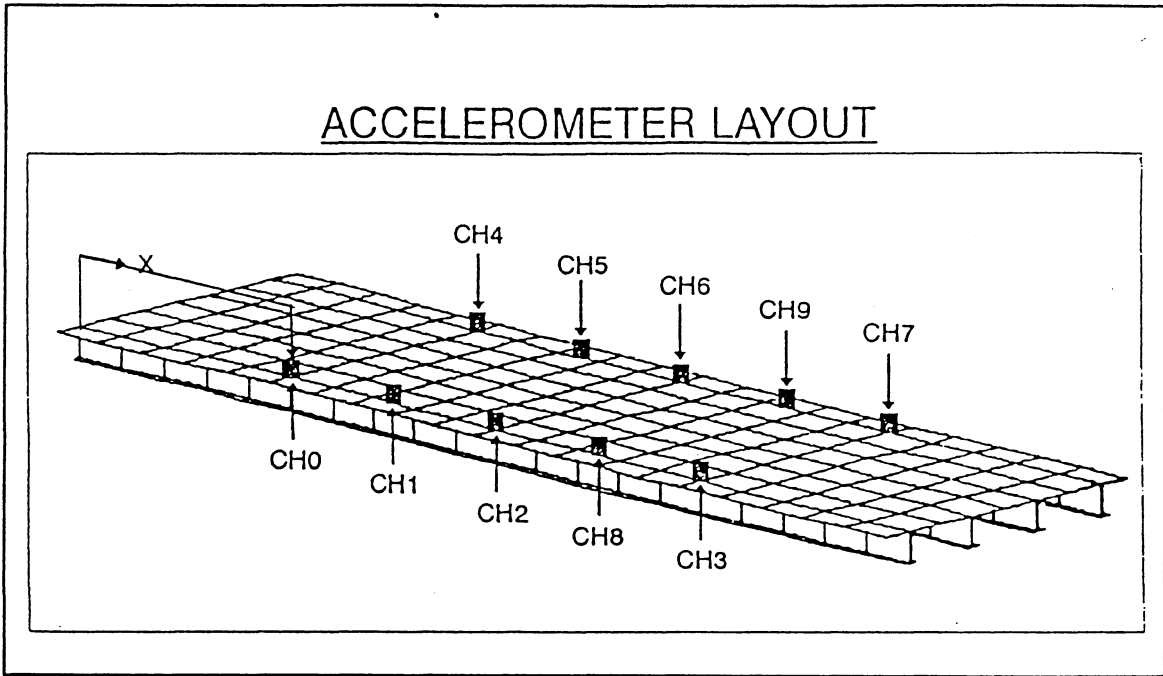


Fig. 3 Instrumentation Layout - Accelerometer Locations

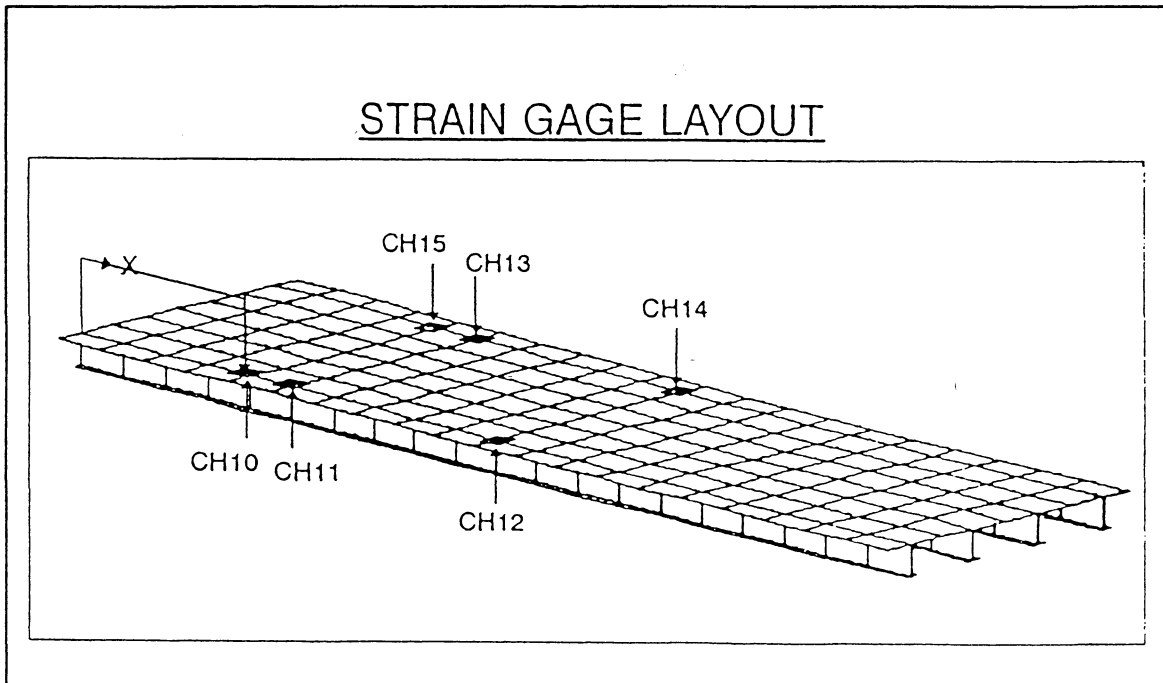


Fig. 4 Instrumentation Layout - Strain Gage Locations

MODE SHAPES AND FREQUENCIES(Hz) FOR MODEL
WITH EXTRA MASTER DEGREES OF FREEDOM

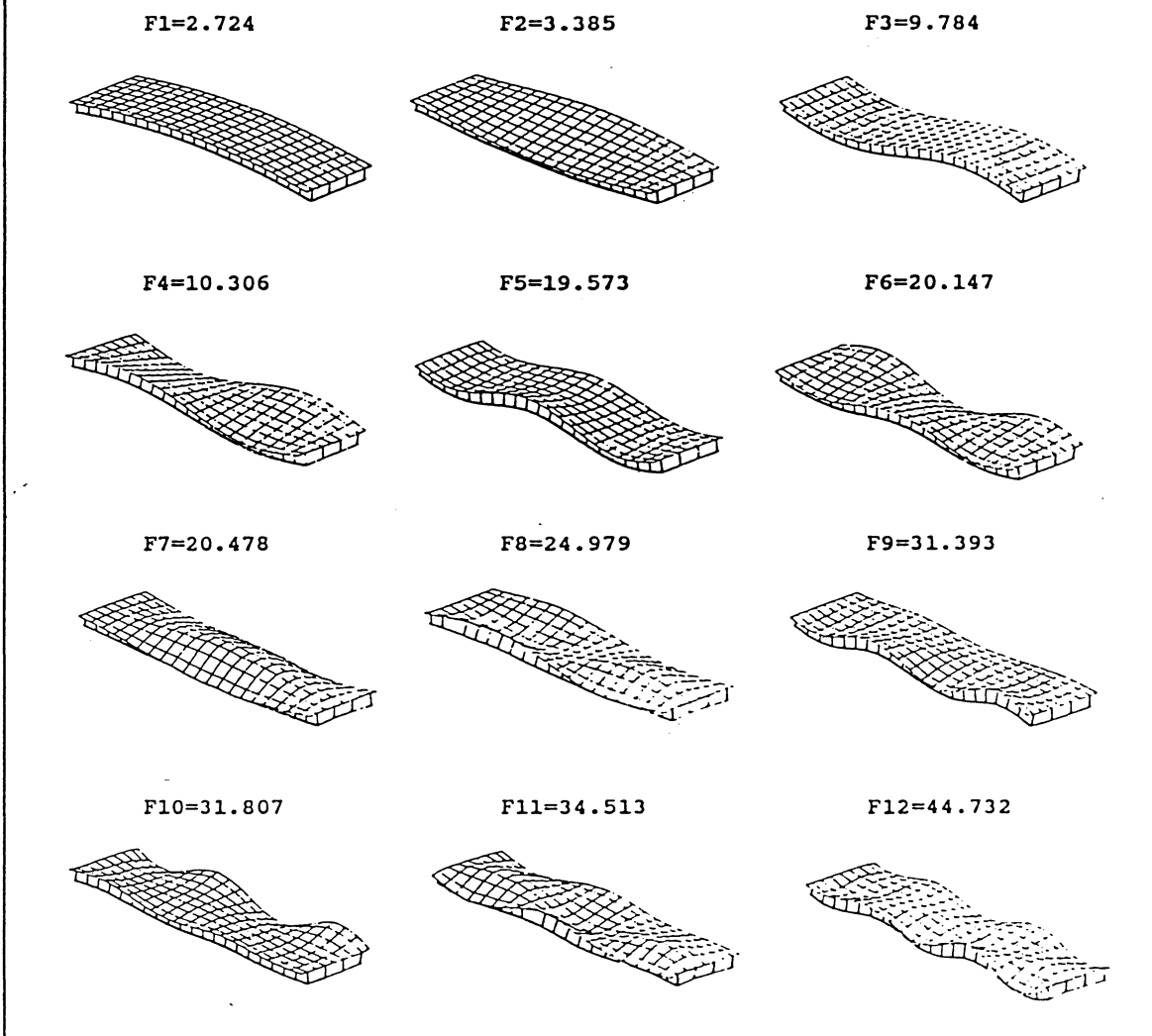


Fig. 5 Frequencies and Mode Shapes from Finite Element Model

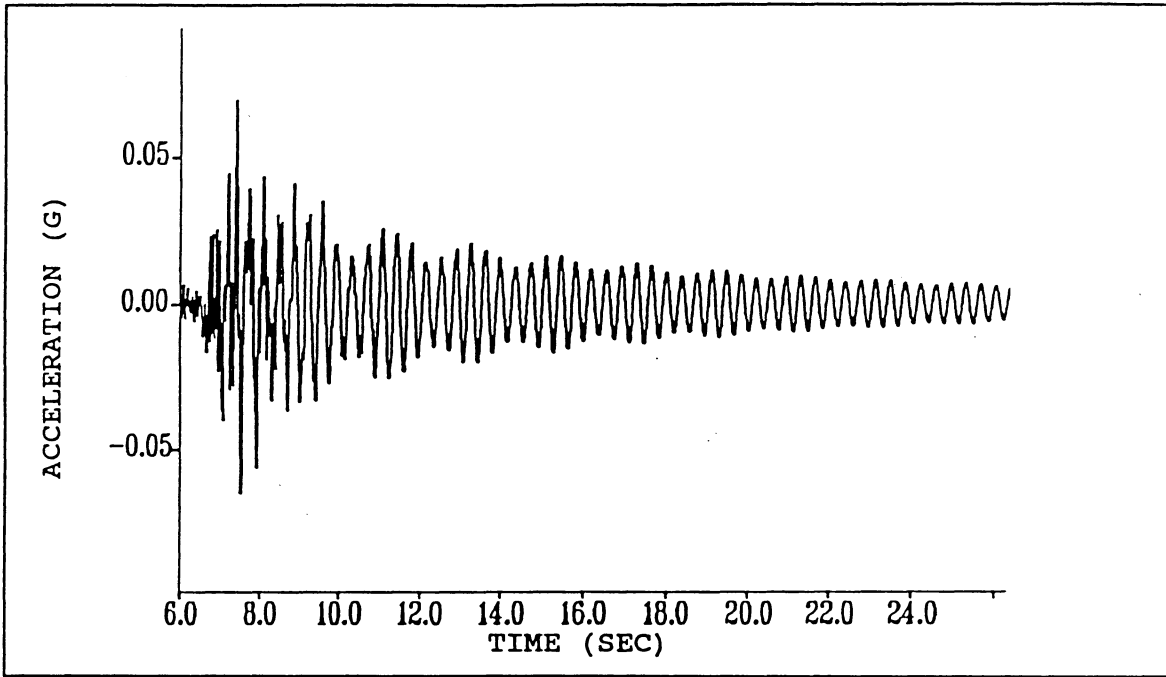


Fig. 6 Typical Accelerometer Time Record (Channel 1)

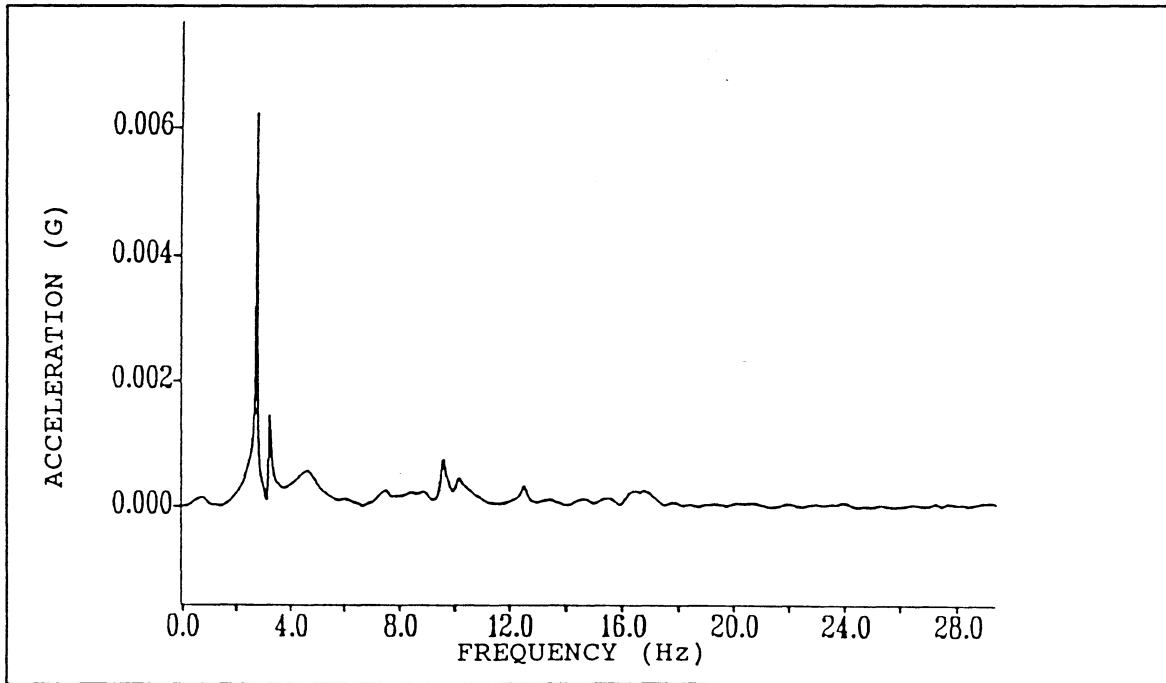


Fig. 7 Frequency Response Plot of Accelerometer Record in Fig. 6

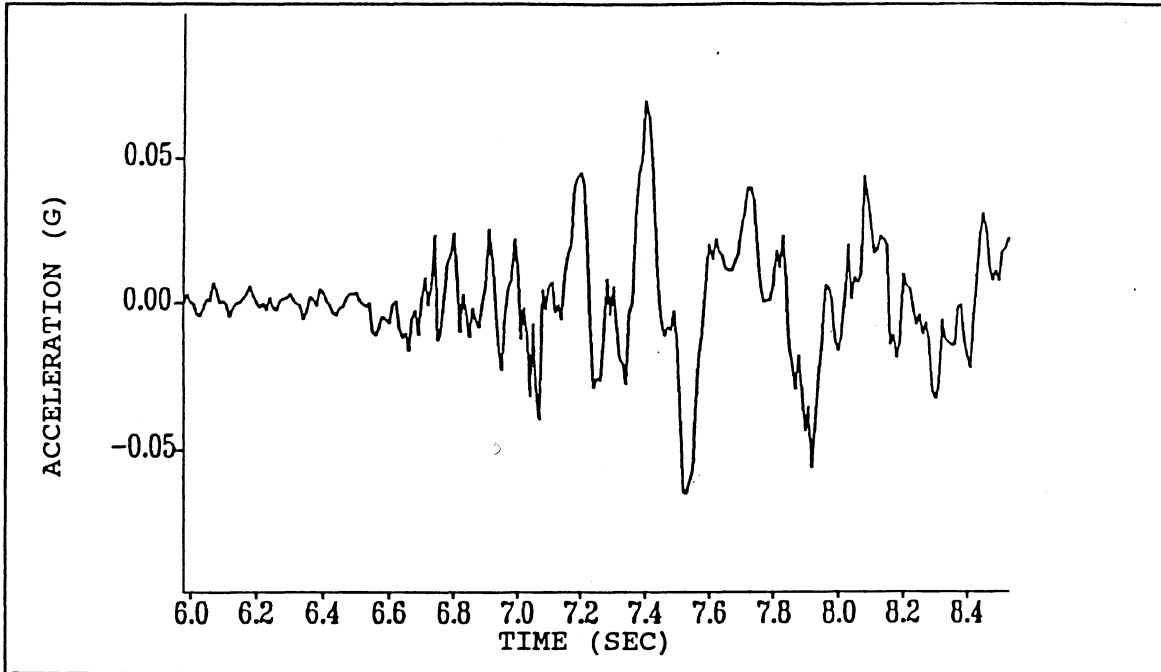


Fig. 8 Accelerometer Record from Channel 1 - Transient Phase

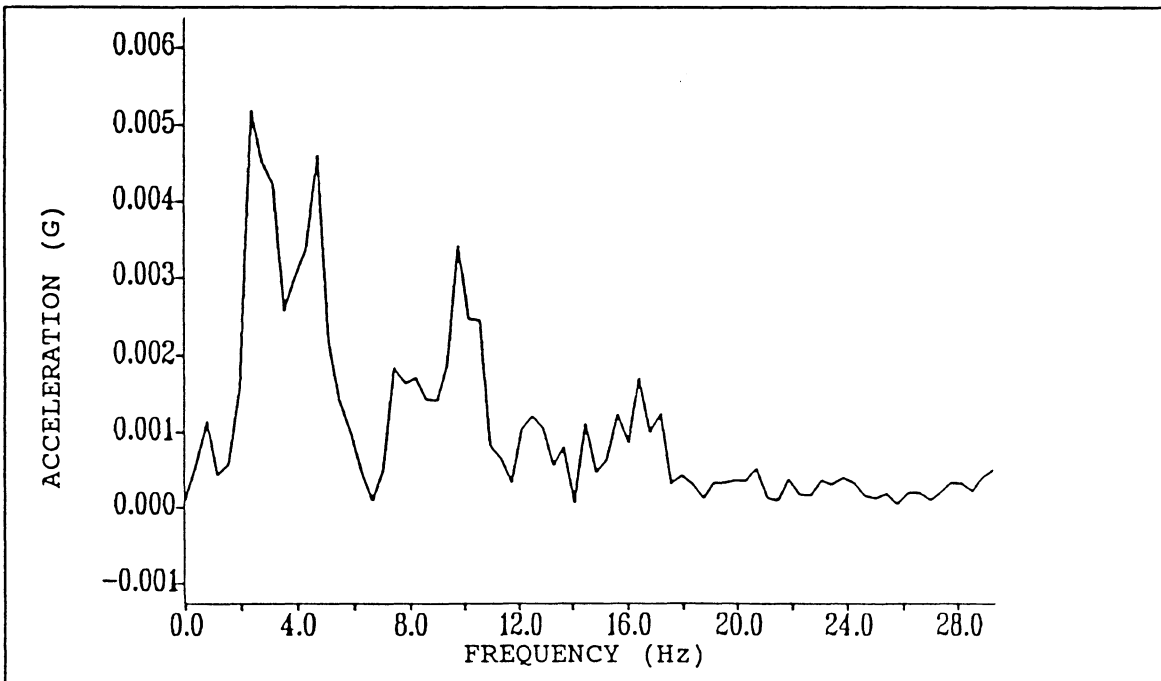


Fig. 9 Frequency Response Plot of Accelerometer Record in Fig. 8

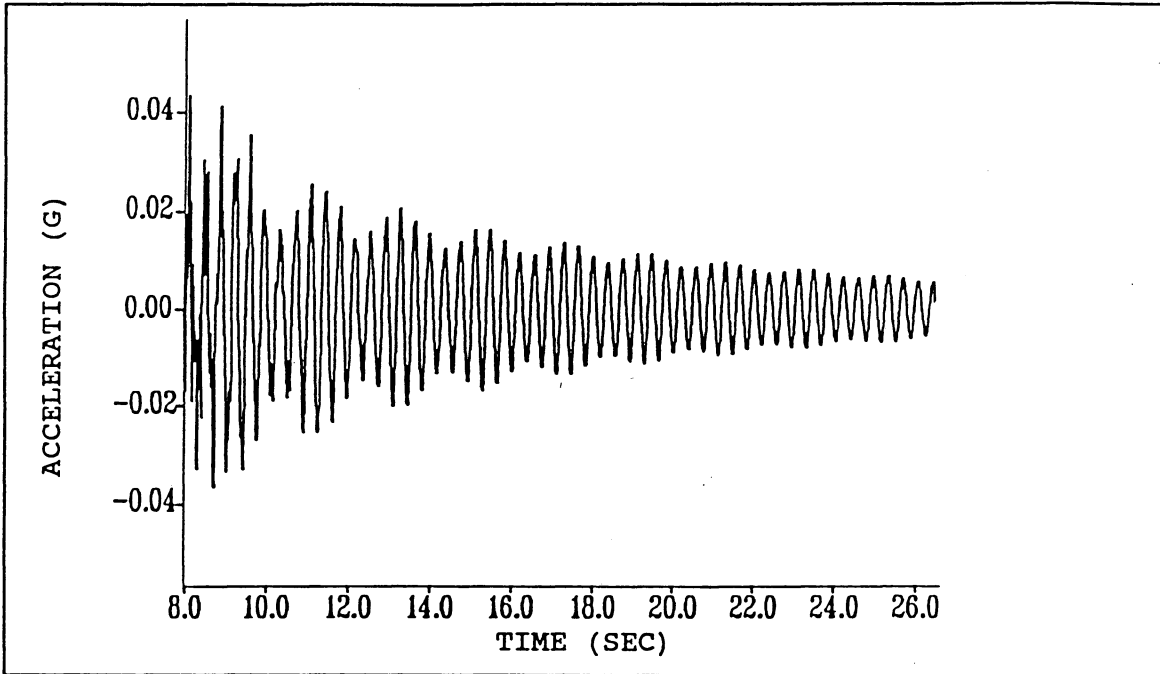


Fig. 10 Accelerometer Record from Channel 1 - Free Vibration Phase

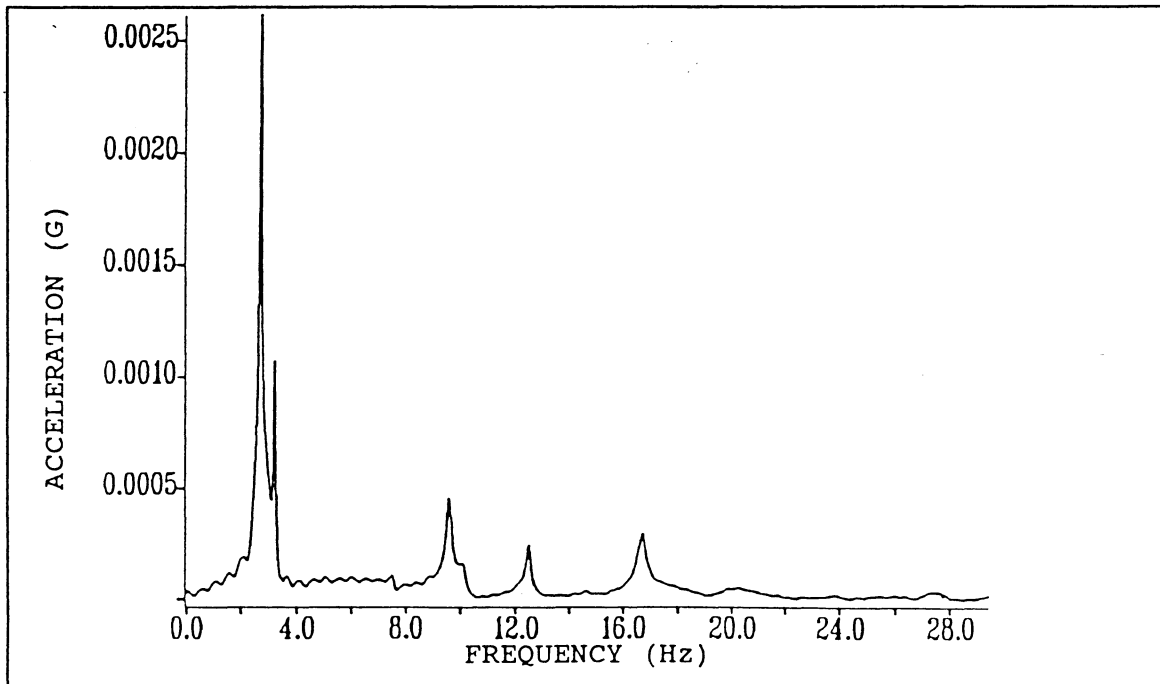


Fig. 11 Frequency Response Plot of Acceleration Record in Fig. 10

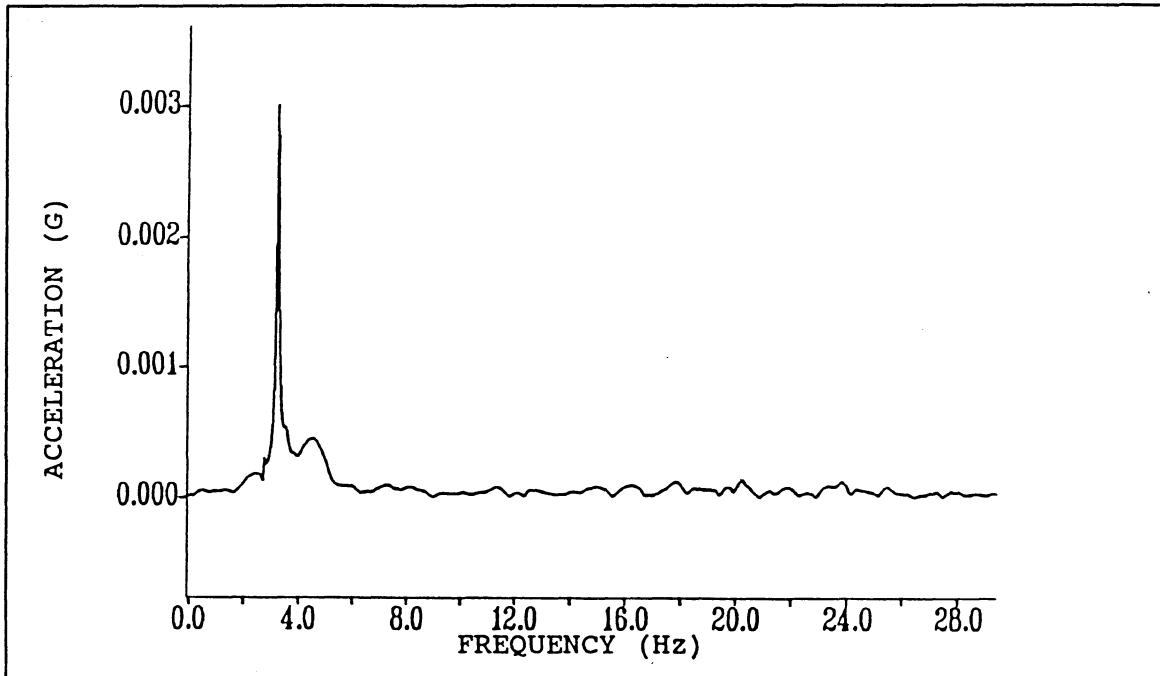


Fig. 12 Frequency Response Plot of Differences in Mid-Span Accelerometer Records

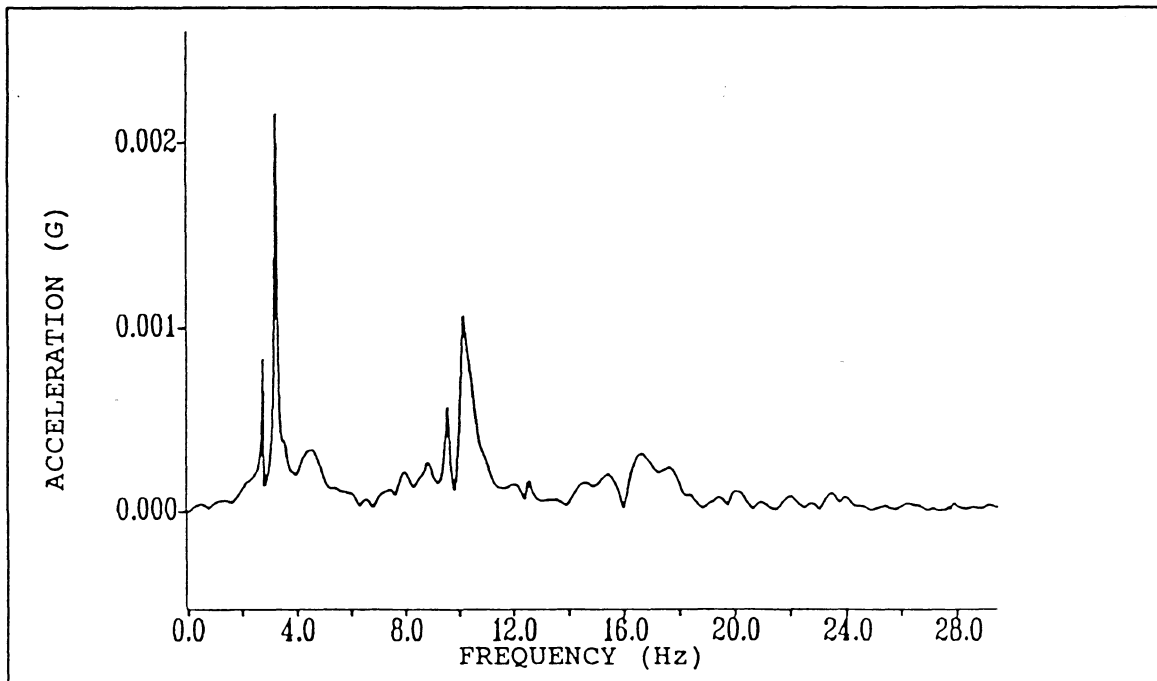


Fig. 13 Frequency Response Plot of Differences in Quarter-Span Accelerometer Records

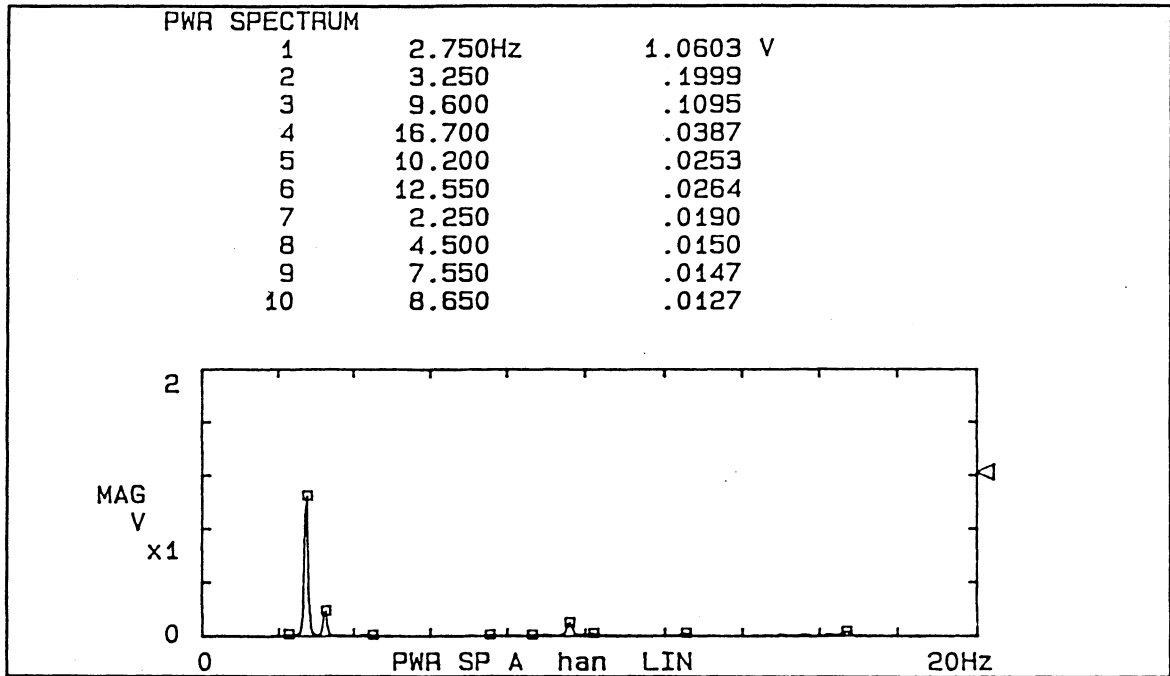


Fig. 14 Frequency Response Plot from Frequency Analyzer - Accelerometer 0

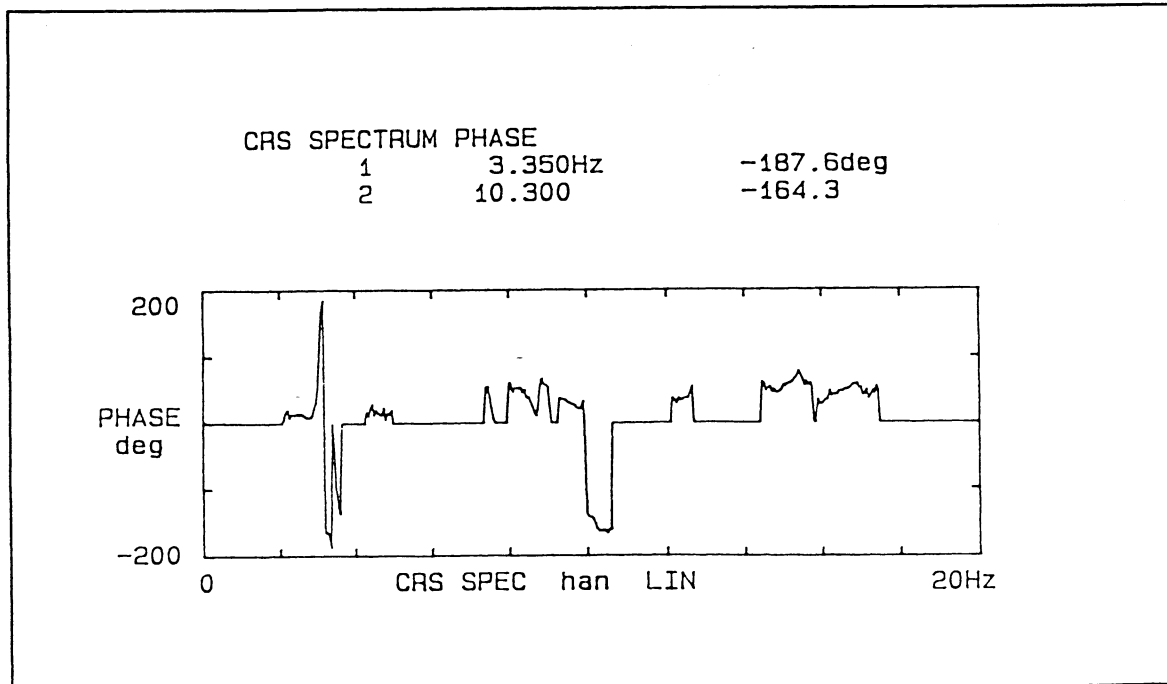


Fig. 15 Cross Spectrum Phase Plot for Quarter-Span Accelerometers

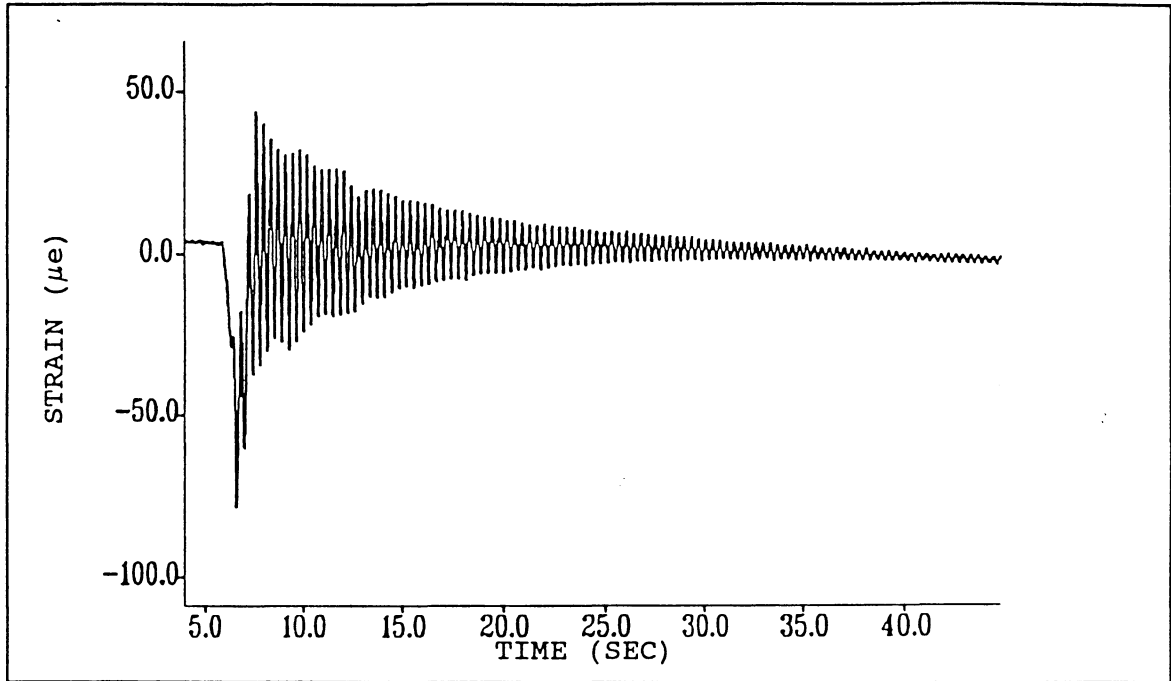


Fig. 16 Recorded Signal from Mid-Span Strain Gage

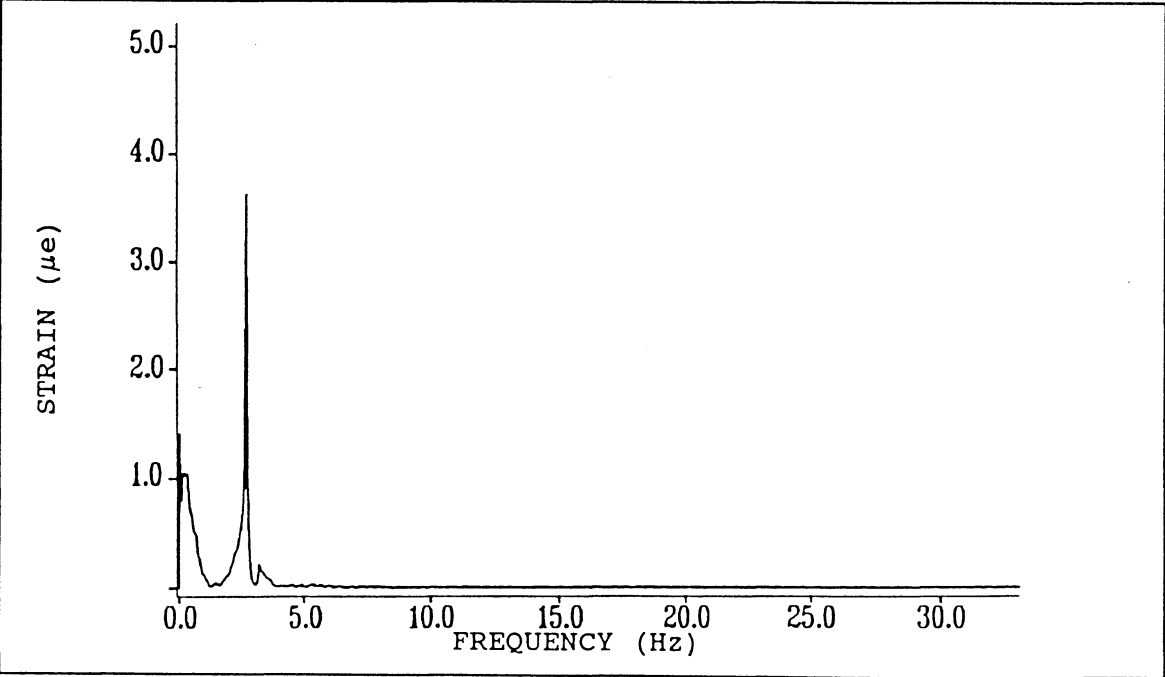


Fig. 17 Frequency Response Plot of Strain Gage Signal in Fig. 16

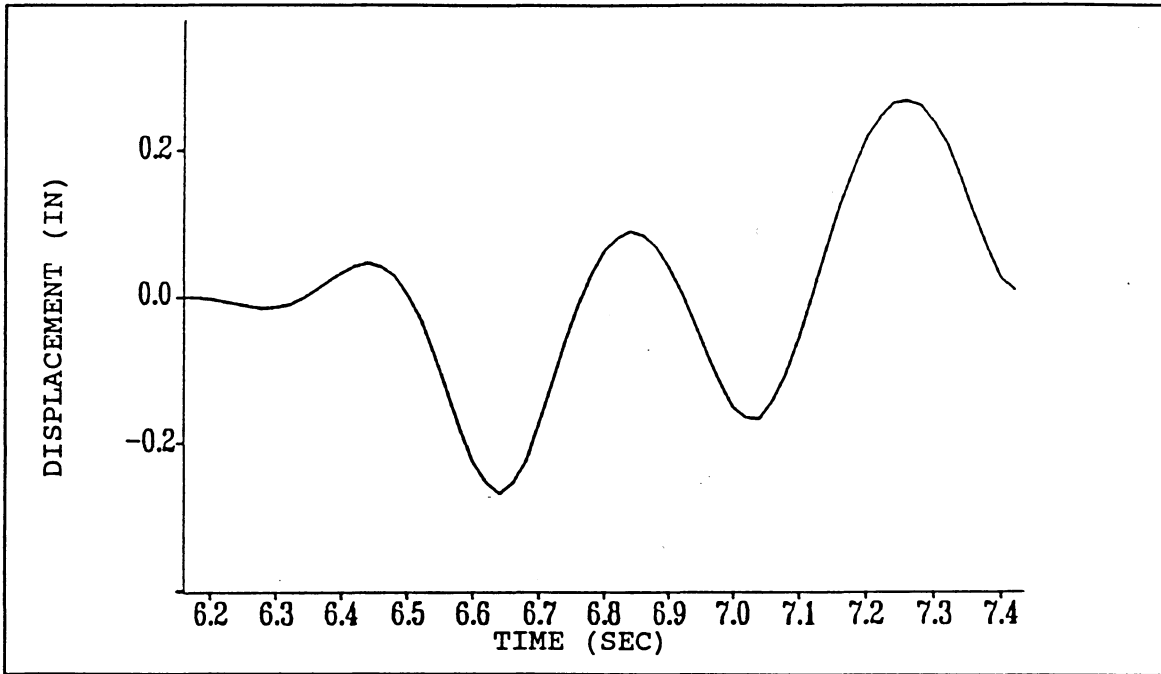


Fig. 18 Displacement Response from Integration of Measured Accelerations

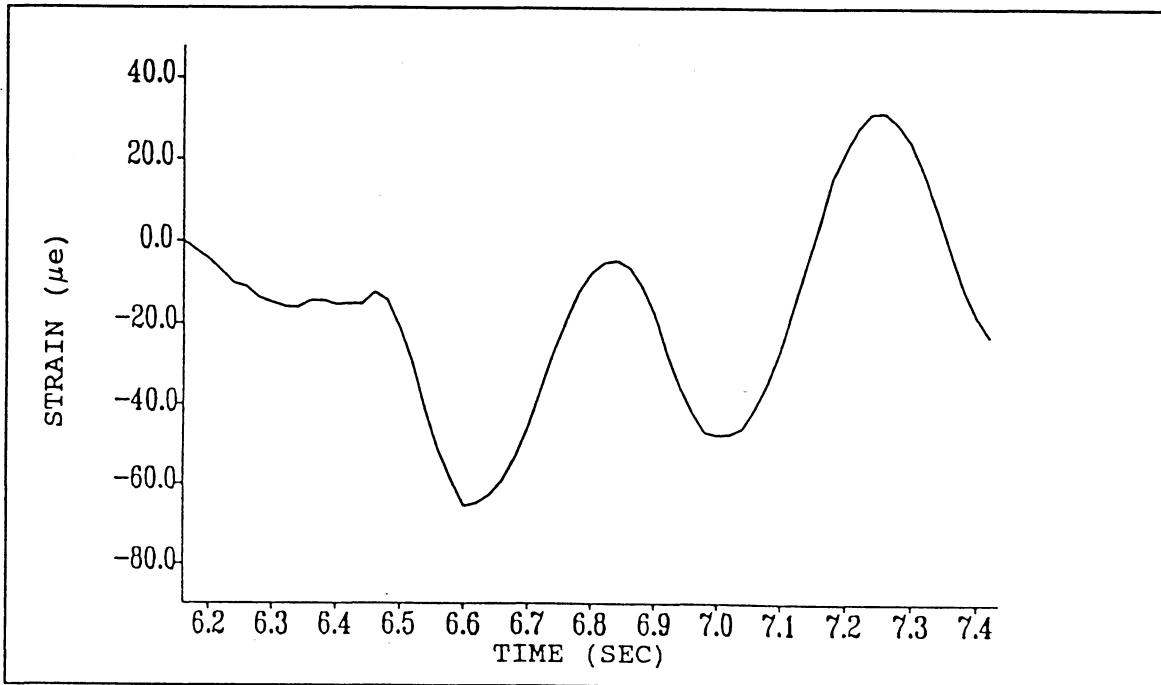


Fig. 19 Strain Gage Response at Same Location as Acceleration in Fig. 18

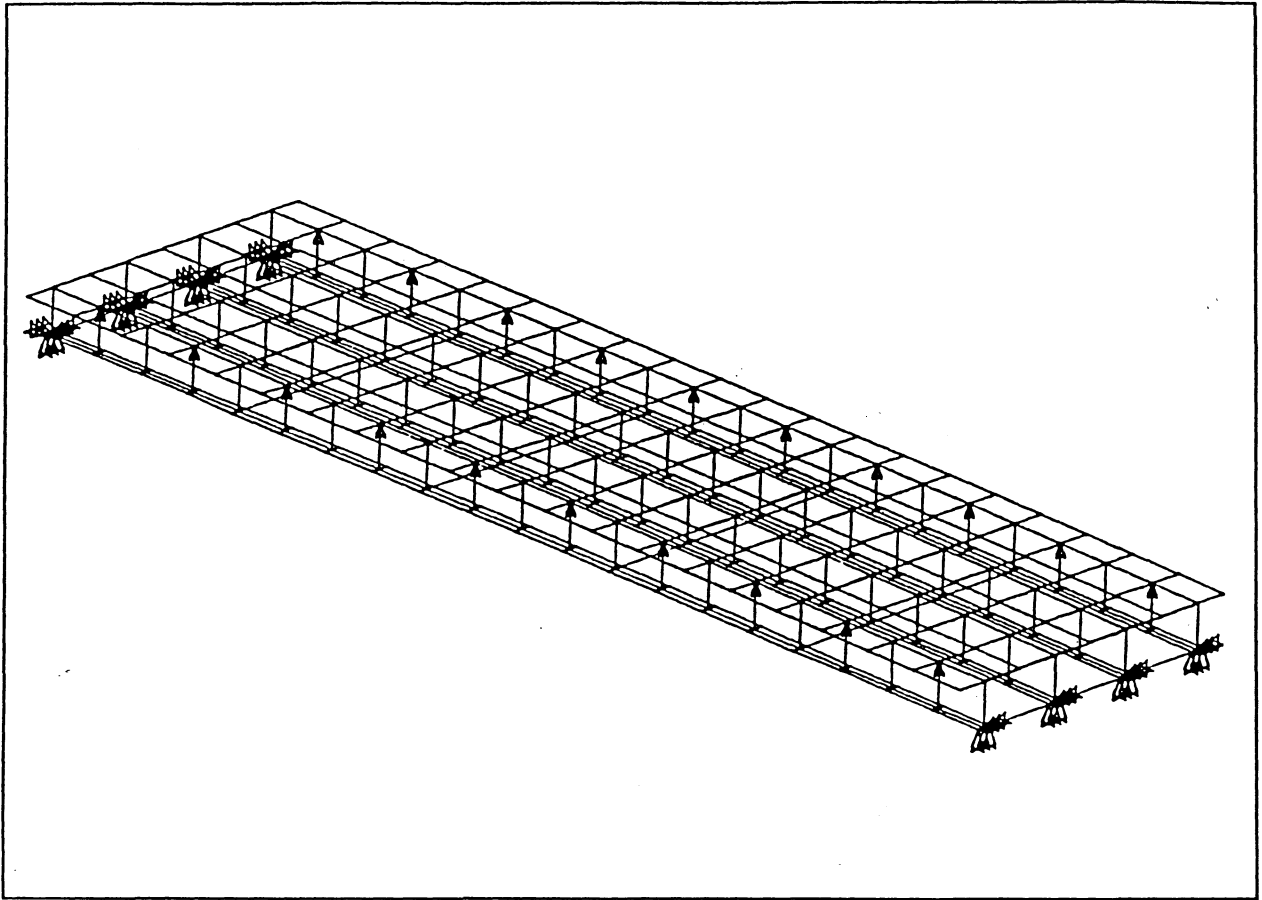


Fig. 20 Finite Element Model of Complete Center Span

MODE SHAPES AND FREQUENCIES (Hz) FOR MODEL
WITHOUT STIFF DIAPHRAGMS

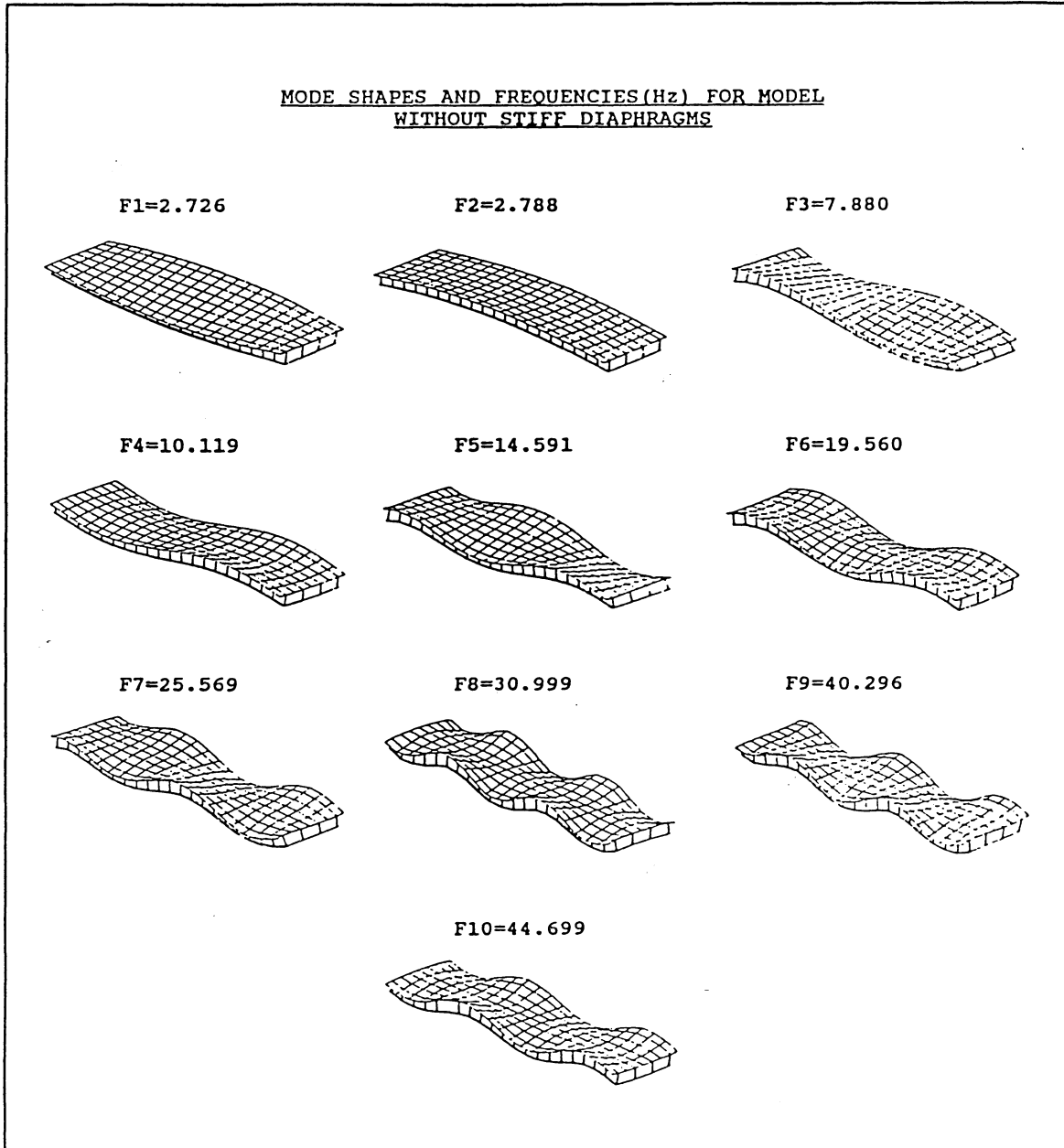
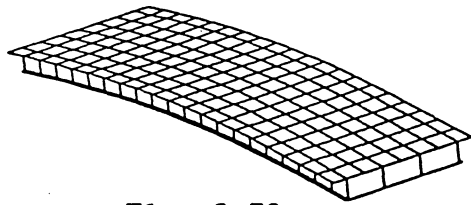
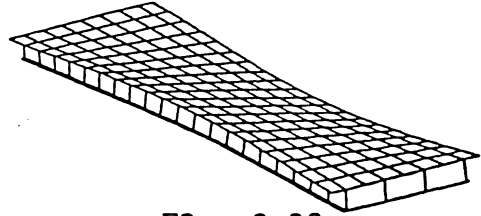


Fig. 21 Calculated Frequencies and Mode Shapes - No Diaphragms

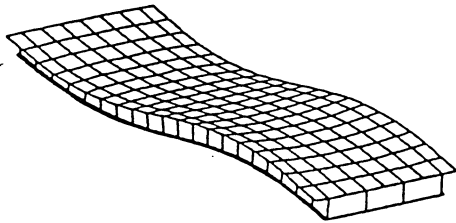
MODE SHAPES AND FREQUENCIES(Hz) FOR BEST MES MODEL
REPRESENTATION OF THE RTE. 58 BRIDGE



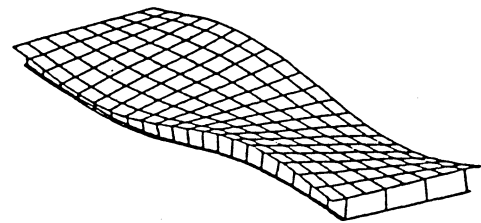
F1 = 2.73



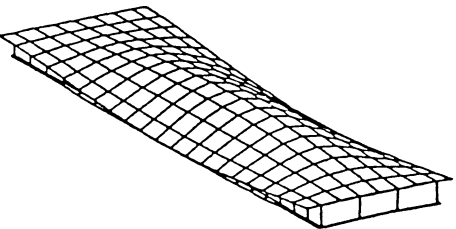
F2 = 3.38



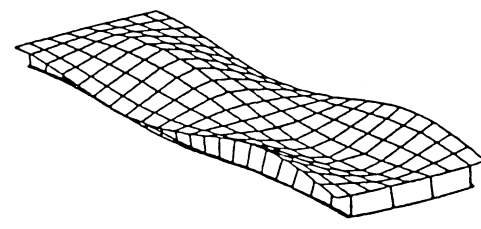
F3 = 9.76



F4 = 10.32



F5 = 12.53



F6 = 18.25

Fig. 22 Calculated Frequencies and Mode Shapes - With Diaphragms

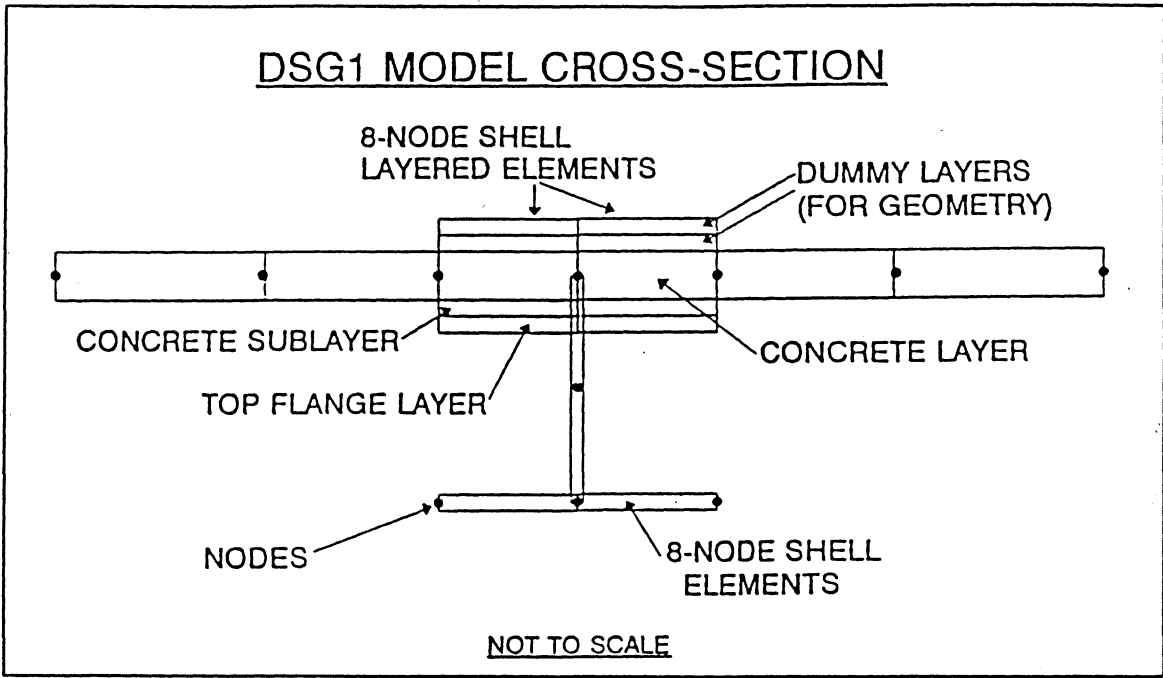


Fig. 23 Detail of DSG1 Finite Element Model

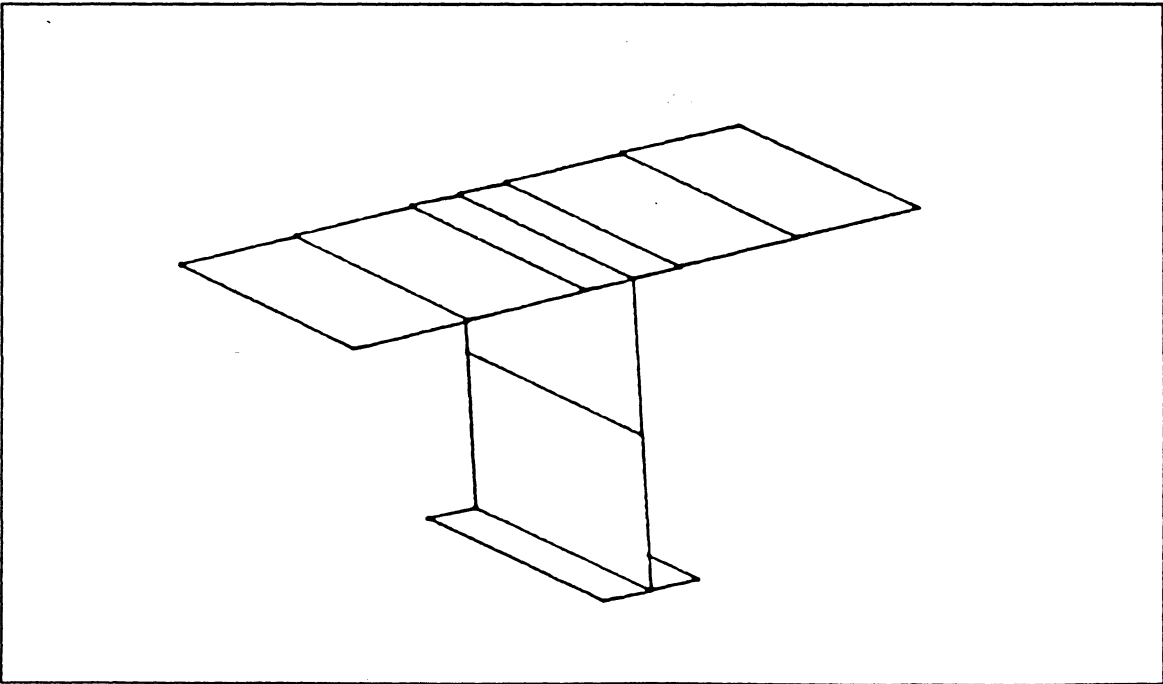


Fig. 24 Connectivity Pattern of SG1 Finite Element Model

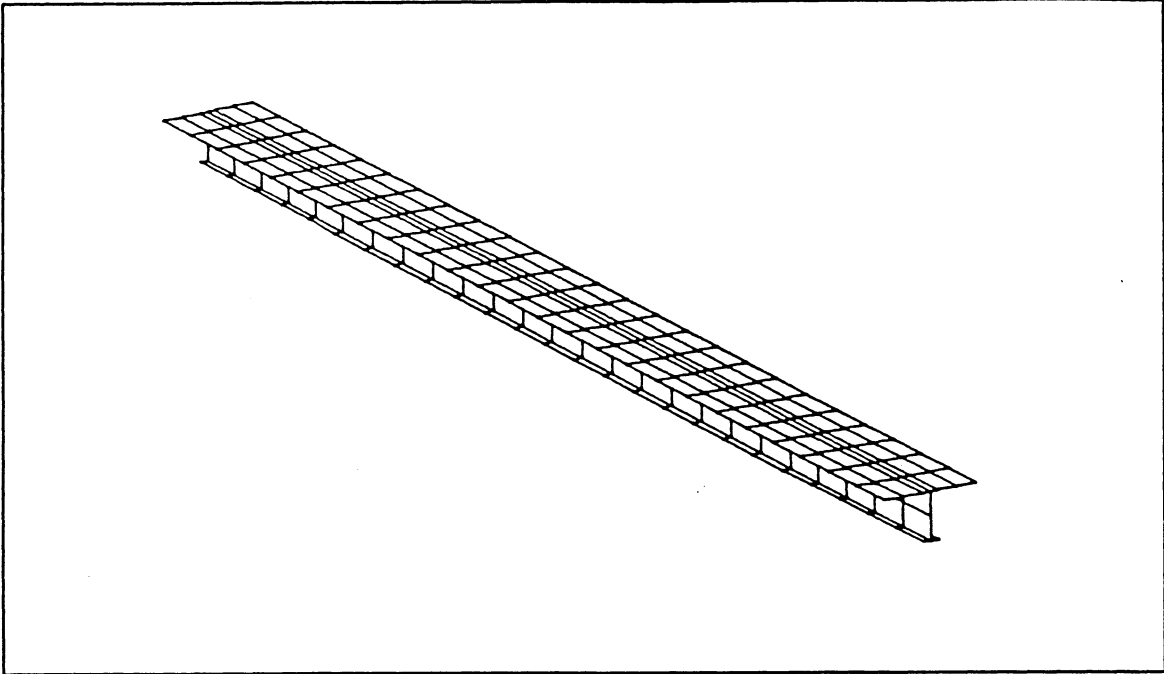


Fig. 25 Finite Element Model of Girder Line

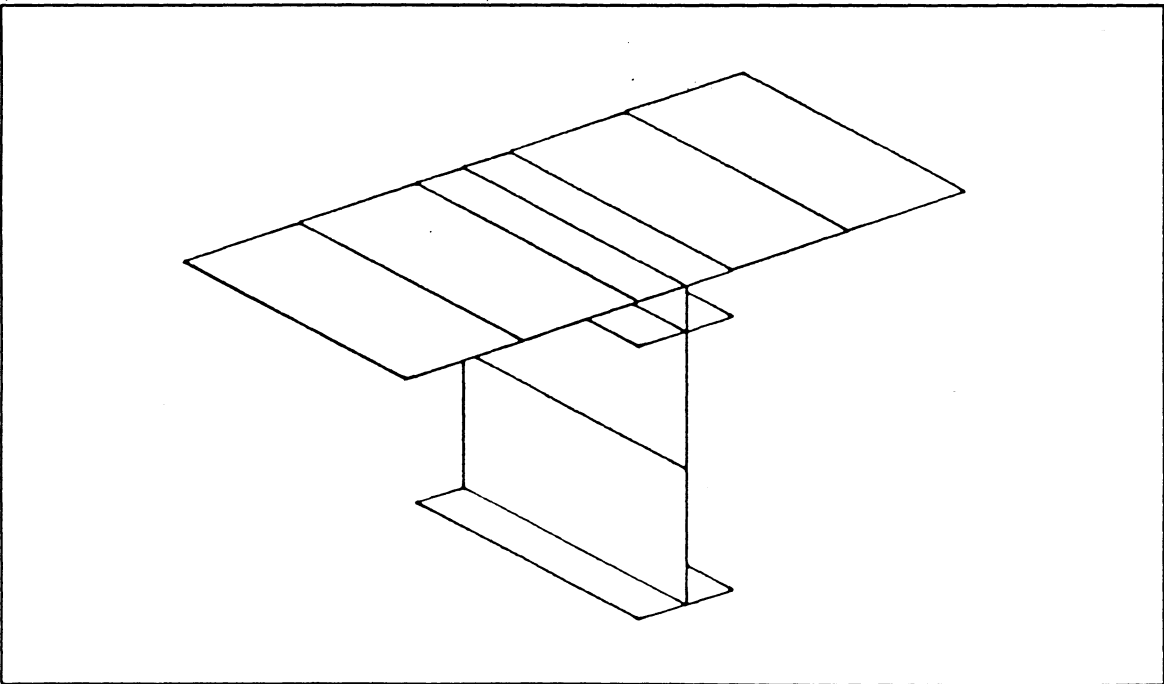


Fig. 26 Connectivity Pattern of SG2 Finite Element Model

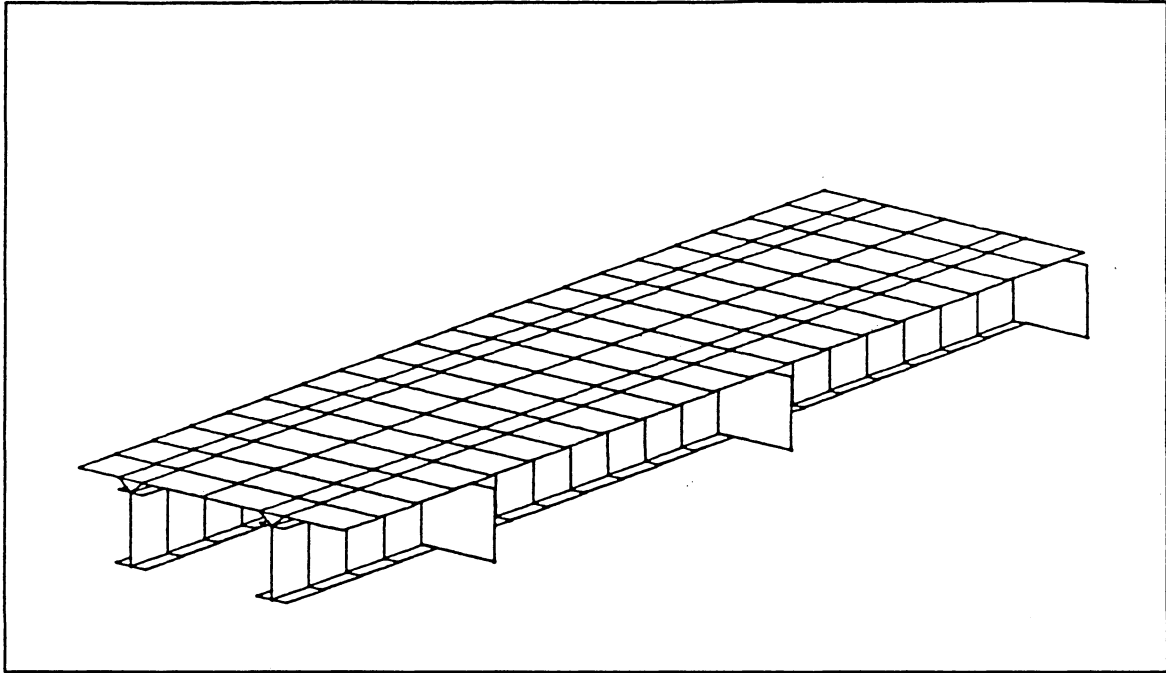


Fig. 27 Finite Element Model of One-Quarter of Bridge (QBM)

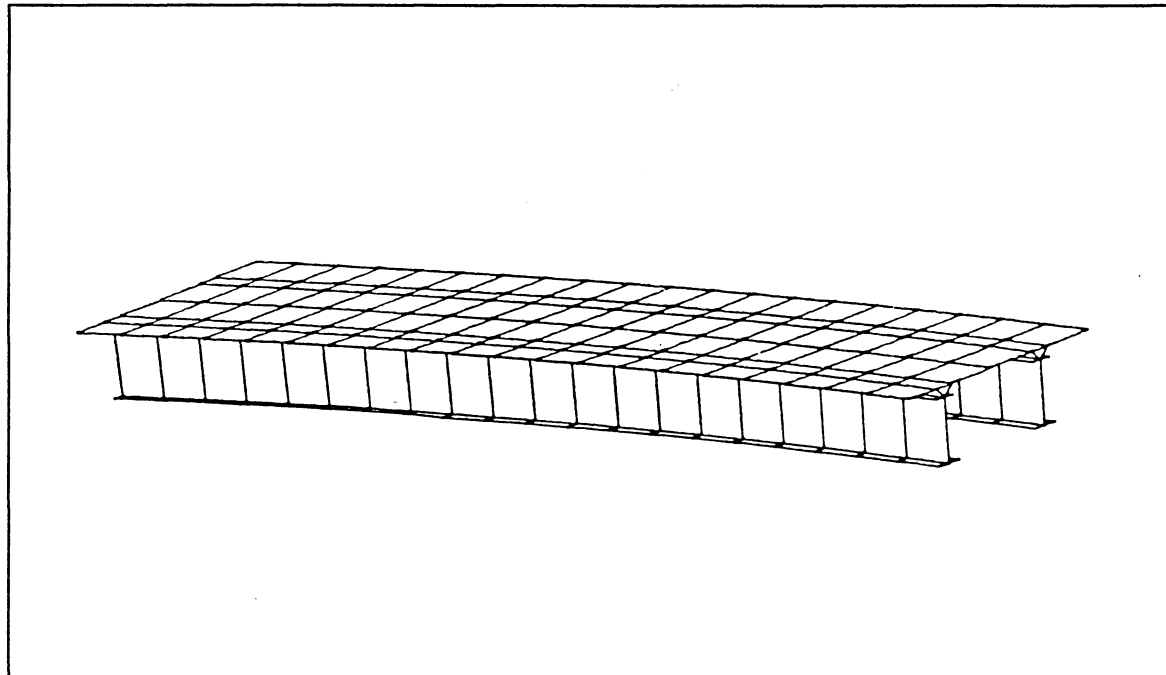


Fig. 28 First Longitudinal Bending Mode Corresponding to Fundamental Frequency (2.7 Hz)

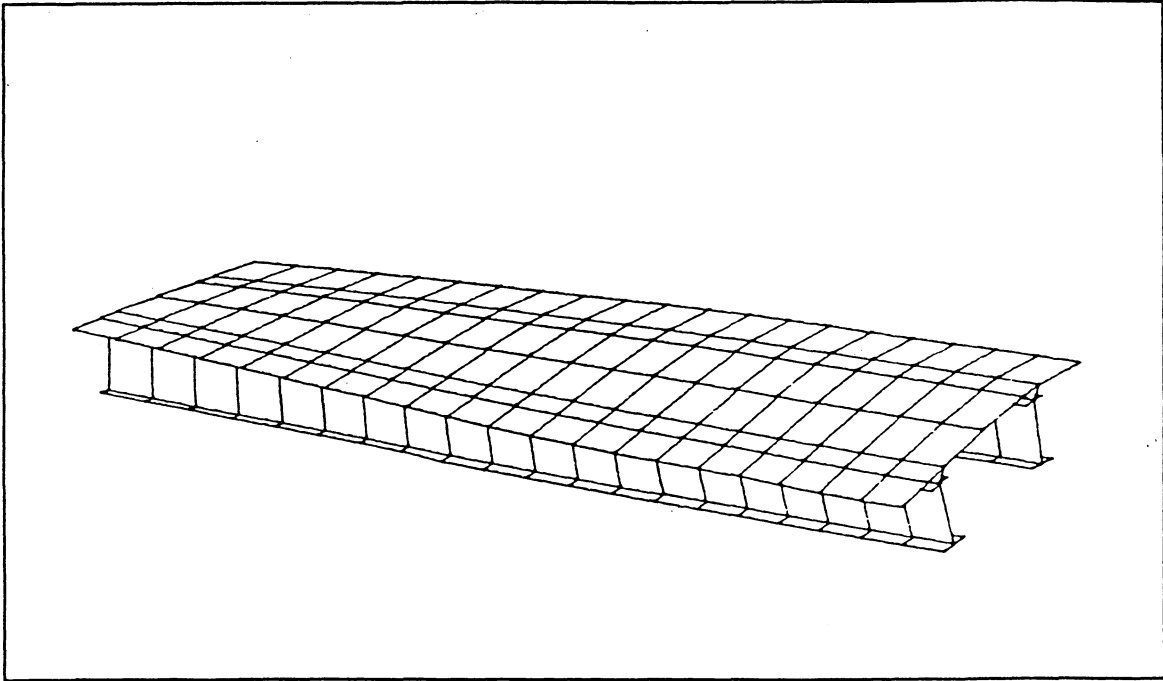


Fig. 29 First Transverse Bending Mode Corresponding to Fifth Natural Frequency (12.5 Hz)

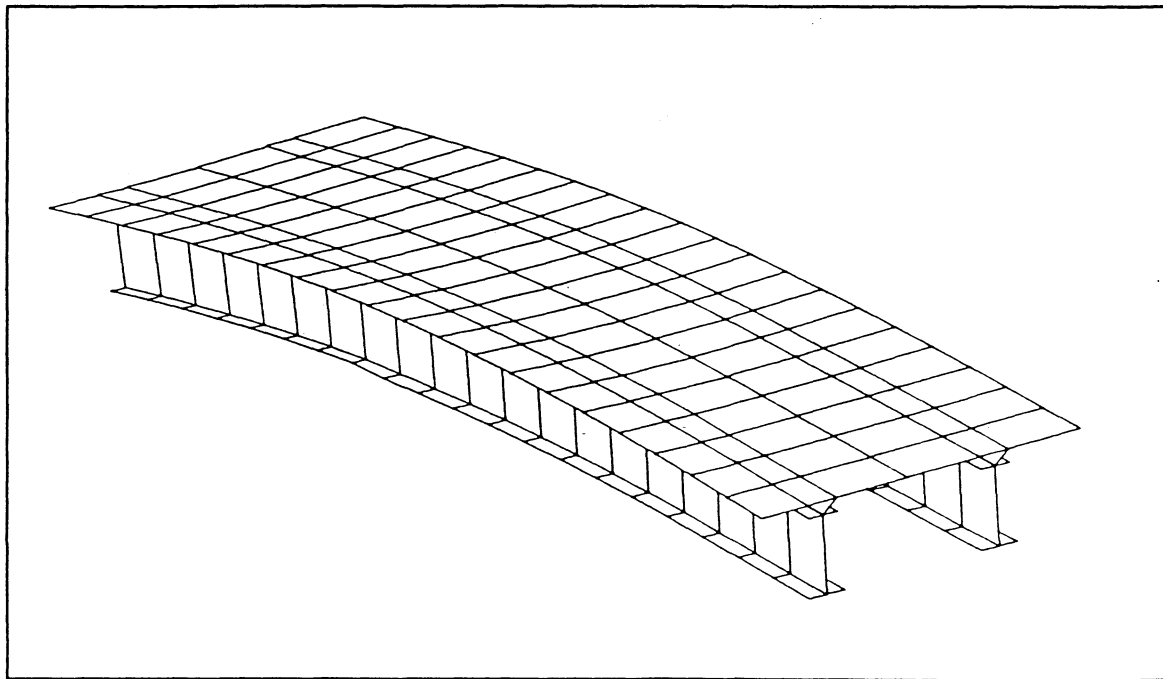


Fig. 30 Second Longitudinal Bending Mode Corresponding to Third Natural Frequency (9.7 Hz)

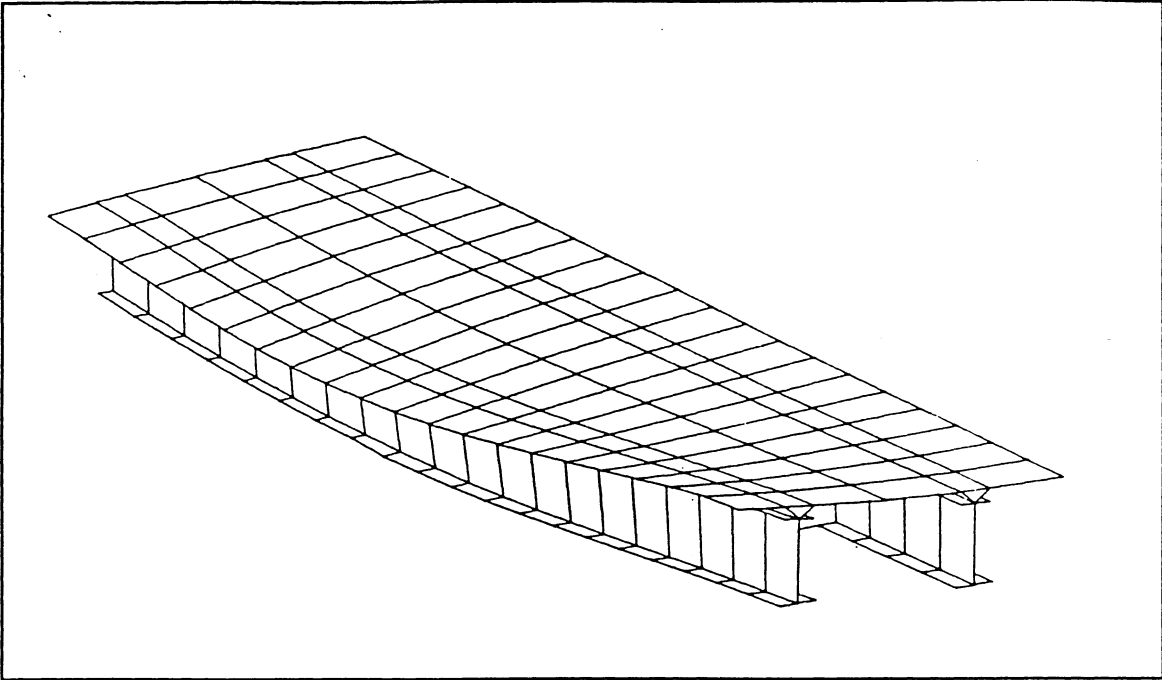


Fig. 31 Mode Shape Corresponding to Sixth Natural Frequency (16.7 Hz)

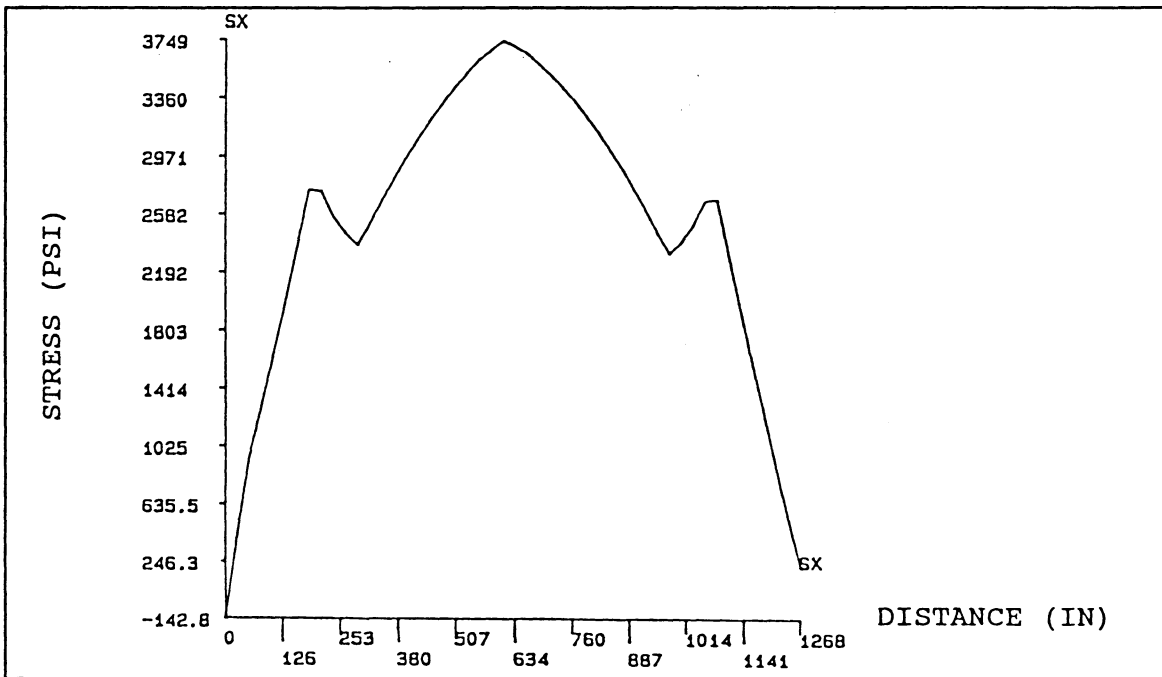


Fig. 32 Bottom Flange Stress Profile - SG1 Model

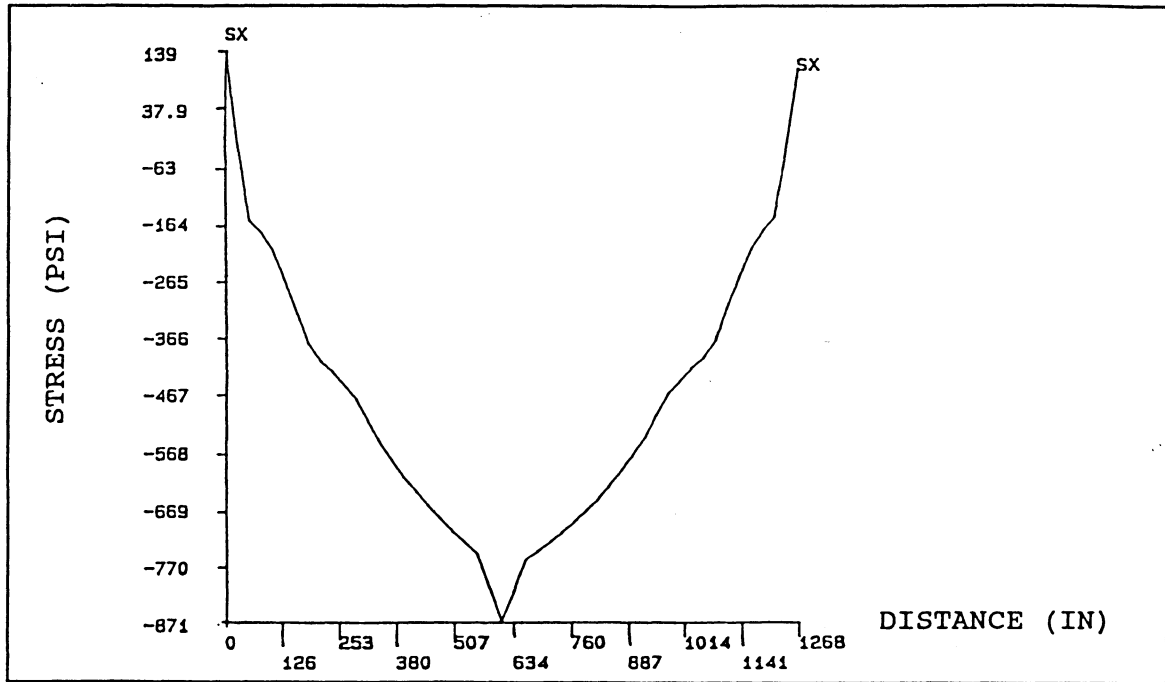


Fig. 33 Deck Stress Profile - SG1 Model

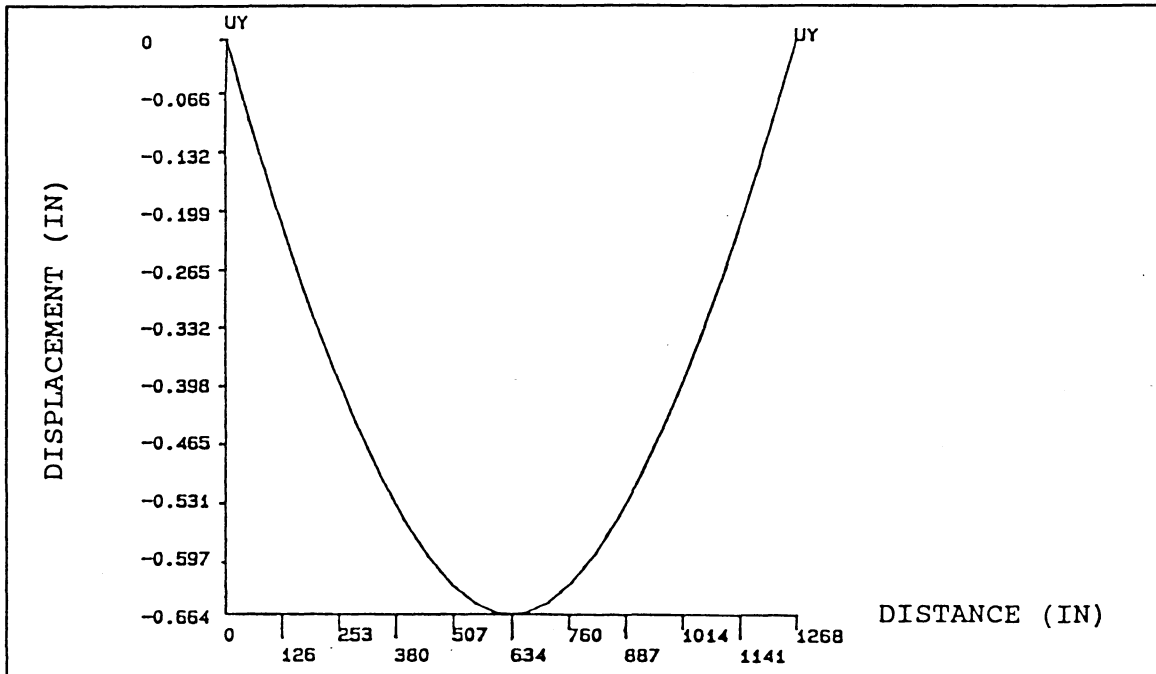


Fig. 34 Displacement Plot - SG1 Model